CRRELEX 93:
Surface Roughness and Physical Properties Measurements

I. H. H. Zabel and K. C. Jezek

BYRD POLAR RESEARCH CENTER
THE OHIO STATE UNIVERSITY

BPRC Technical Note Number 93-02

Byrd Polar Research Center
The Ohio State University
Columbus, Ohio 43210

CRRELEX 93:

Surface Roughness and Physical Properties Measurements

I. H. H. Zabel and K. C. Jezek

Byrd Polar Research Center

The Ohio State University

Columbus, Ohio 43210

I. Introduction

In this report we describe the measurements we made on saline ice at CRREL during January 1993, and we discuss some preliminary results and interpretations. In addition, we discuss directions to take regarding analysis of this year's CRREL data, and ideas for future work.

We obtained extensive surface roughness and physical properties data using a variety of instruments and techniques, particularly for the ice grown indoors in the pit. We took care to take measurements in conjunction with the radar measurements taken by the University of Kansas group in the pit, so that the radar and physical properties data could be meaningfully combined. Outdoors, we also tried to take data in regions of the pond and at times that coincided with the passive and active microwave measurements being made by various groups.

This report is divided as follows: we describe our surface roughness measurements for both the pit and the pond in Section 2, and salinity and structure measurements in Section 3. In Section 4 we discuss our findings, and in Section 5 we discuss future work.

II. Surface Roughness

A. Instrumentation

Our aim was to measure the surface roughness of the ice at all stages of growth, and for all roughness regimes, including both the natural and

artificially-applied roughness. In order to do this, we designed and constructed a new mechanical roughness gauge. The novel features of this gauge were that it could operate on thin (i.e. 2 mm thick), fragile ice, and that it obtained four linear samples simultaneously, in two perpendicular directions. Prasad Gogineni also contributed to the design of the gauge, which is shown in Figure 1.

Conventional mechanical gauges with a resolution fine enough to probe the roughness that exists on thin ice obtain one linear roughness transect, and must be pushed down firmly onto the ice. This almost invariably leads to gouging into the ice, which destroys the surface, and can also cut through thin ice entirely. Optical methods employed by other groups involved either cutting out a slab of ice or placing heavy instruments on the ice, and so were also intractable for thin ice measurements. Our gauge was constructed out of lightweight materials, and the rods which probed the surface height could be moved up and down without much force – yet remain in place after a measurement was completed – so that they did not cut into the surface. In addition, the instrument's weight was spread out by having the rods form a rectangle rather than one line, and by padding at the end of each rod.

We were able to measure vertical roughness at length scales from a few tenths of a millimeter to on the order of a few centimeters. At the lower end of this roughness scale one approaches the noise level of the instrument, so the measurements become less accurate. The limitations of our instrument were that the length of each transect was shorter than is ideal: the long sides were about 22 cm long, and the short sides only about 9 cm long. In

addition, the spacing between rods was 2.5 mm, so we could not discern roughness at length scales smaller than this horizontally. When possible and useful, we used two other mechanical roughness gauges which had either finer resolution or a longer span. One such instrument was a six-inch-long metal contour gauge, several of which could be bolted together to form a long gauge, and which consisted of the same rods as in our lightweight comb gauge, but more tightly packed (see Figure 2). These metal gauges most often cut into the ice surface, but were useful for large-scale roughness such as that obtained when we spread ice cubes on the ice surface. We also used a large, long gauge with rods spaced 1 cm apart to look at large scale roughness (Figure 3).

With all the roughness gauges except the large one, our procedure was to make the measurement, photograph the gauge as well as hand trace the contours formed on the gauge by the surface, and then digitize and process the hand traces. In real time we could thus extract a surface height profile, r.m.s. roughness of the profile, correlation function, and correlation length (Figure 4). These results are preliminary and presumably less precise than the digitization of the photographs to follow. Our real time analysis was useful, however, as a consistency check on the qualitative behavior of the Kansas group's radar returns, and for determining what type and scale of roughness we achieved in the various artificial roughening attempts.

B. Indoor Ice

The indoor pit was divided into two sides: the far side, where the pumps were located and where pancake ice formed initially (Figure 5), and the near side, where the ice formed a smooth sheet initially (Figure 6). We focused on the near side, where radar data was taken, until the later phases of the roughening experiment, which were done on the far side.

Table I shows preliminary roughness statistics from hand traces of the indoor ice surface, averaged over as many samples as possible, and only for the long sides of the lightweight roughness gauge. Much work remains to be done in terms of processing the photographs for all the roughness gauges, and averaging the data. The preliminary results show, however, a gradual, natural roughening of the surface as the ice thickened.

After the ice had grown to about 19 cm thickness (Figure 7), we attempted to artificially roughen the surface in several ways. First, we sifted a snow layer onto the near side ice. The layer was densely covered with snow, and on the order of a centimeter thick (Figures 8,9). This created a surface which had some visible large-scale roughness horizontally, but which was extremely difficult to characterize by mechanical means. In addition, the snow cover wicked up brine, creating a dielectric "roughness" which was also hard to characterize (see section 3). We collected a roughness transect with the large comb gauge which remains to be processed, but we felt that this attempt at roughening was unsuccesful in terms of creating a surface with well-characterized properties that could be meaningfully incorporated into models to explain the radar data.

We next spread a densely-packed layer of uniformly-sized ice cubes onto the far side of the ice, and sprayed a light mist of water onto the surface (Figure 10). After about a day of measurements, we applied a thicker coating of water, in order to fill in air spaces between the cubes that led to volume scatter (Figure 11). Table I shows preliminary roughness statistics for these surfaces. Although the roughness is larger, all of the roughness length scales measured in the pit are small enough with respect to the wavelength at Ku band to suggest that the small perturbation model should provide a better description of surface scattering than the Kirchoff scalar or stationary phase approximations.

C. Pond Ice

We measured the surface roughness of the pond ice in its smooth, natural state (Figure 12), and also after the surface had been roughened artificially. Due to warm weather, the ice outdoors did not grow rapidly (Figure 13). However, a decision was made when the ice was about 7-8 cm thick to artificially roughen the surface.

First, a thin, sparse layer of snow was applied to part of the surface (Figures 14,15). This layer consolidated well with the ice, although warm temperatures led to a persistent wetness and sometimes slushiness during the days. For a second roughness regime, we applied a sparse layer of crushed ice cubes on top of the snow-roughened surface (Figures 16,17), which by this time appeared to have smoothed somewhat, presumably due to melting. Our experience indoors showed that the dense layer of uniformly-sized ice cubes

led to non-Gaussian and occasionally bimodal height distributions. This suggested application of a variety of particle sizes, obtained by crushing. By applying a sparse layer we avoided creating air pockets between particles. We measured the roughness of this surface both with the lightweight gauge and a string of four of the metal gauges; these data remain to be processed.

III. Salinity and Structure

A. Indoor Ice

We measured salinity profiles of the ice as it grew. We generated profiles by removing slabs of ice, sawing off slices of the slab with depth, melting the samples and measuring the salinity with a conductivity bridge or an optical refractometer. Much of this work was done by or together with Tony Gow. Several results are shown in Figures 18-21. One sample was processed with Tom Grenfell's slicing method, where sections of a slab are sliced simultaneously by rubbing the slab against sharp blades; the ice then falls into evenly spaced bins where it melts and can be sampled bin by bin for salinity. In addition, we have several salinity measurements of the snow layer which was deposited to roughen the surface. Samples were scraped from the surface along several transects (Figures 22,23), but we had no satisfactory method of measuring the salinity of the snow with depth.

Structurally, we observed the formation and alignment of crystals as the ice grew. Large frost flowers formed in between the two sides of the pit; smaller frost flowers covered the far side of the pit after about a week of

growth (Figure 24). Undisturbed portions of the slabs used for salinity sampling were retained for making thin sections; most of this work remains to be done.

B. Outdoor Ice

Several slabs of ice were taken for salinity and structure measurements on the outdoor ice; most of our physical properties work, however, focused on obtaining surface and near-surface salinities. This was mainly because of the persistent melting,refreezing, and light snow deposition on the surface: we wanted to characterize the salinity of the surface through all these changes.

We obtained most of the surface scrapings with a device of Tom Grenfell's. This consisted of a set of 5 blades on blocks and stabilized within a metal frame which allowed one to sample to a depth of 5 mm from the surface, one millimeter at a time. Other samples were scraped off the surface in a more crude manner, with a flat instrument such as a metal plate or ruler. Several results are shown in Figures 25-27. The surface varied from wet and slushy during the days to hard at night.

Finally, we extracted several slabs and microtomed off scrapings every millimeter, down to a depth of 3 cm. Figure 28 shows the salinity vs. depth for two samples, one from the unroughened surface of the pond on Jan. 27, and one from a patch of the snow-roughened surface, on Jan. 30. The salinities are near constant below several mm of depth; this might indicate that brine was wicked up from deep down in the ice to the surface, with an even salinity distribution as it moved upward. The sample from Jan.

30 showed many air bubbles upon visual inspection; we have yet to obtain photos of thin sections or salinity profiles from deeper in the sample.

IV. Discussion

During the 1993 experiments at CRREL, we made a thorough investigation of the indoor and outdoor ice physical properties, including surface roughness, salinity, and structure. Much analysis remains to be done, such as careful compilation of surface roughness statistics and estimation of the uncertainty in our roughness measurements. Thin sections from ice slabs in cold storage must be cut, photographed, and the microscopic structure analyzed. We hope to incorporate data on brine and air volume fraction and inclusion shape and size as a function of time into various scattering models. Finally, salinities from depths below 3 cm in the outdoor ice would be useful for comparison with the near-surface salinities, to determine the direction and manner of brine flow.

Combining the radar and physical properties data presents several challenges. The indoor ice remained quite smooth and uniform until the artificial roughening experiment, and was allowed to grow to around 20 cm thickness before the roughening phase began. This thickness assures us that the radar was not penetrating to the ice-water interface, and thus the effects of roughening the top surface should be clearly evident in the radar return. The types of surface roughness achieved, however, were either difficult to characterize (the snow-roughened case), or most likely non-Gaussian distributed (Figure 29) and perhaps forming a volume-scattering surface layer (the ice

cube case).

Outdoors, we attempted to create rough surfaces that were easier to characterize; this appears to have been successful, although it is not yet clear if the height distributions show simple Gaussian behavior. Interpretation of the radar and passive microwave results will be problematic in any case, however, because the ice only grew to about 7-8 cm before we applied the roughness, so that emission and scattering from the ice-water interface may affect the measurements. We were unable to measure the roughness of this interface. In addition, the ice went through strong thermal cycling, with daytime melting and nightime refreezing that most likely affected the salinity and structure in some complicated way. Occasional light snowfalls added fresh water to the ice. Analysis of the cores and salinity scrapings collected outdoors will aid in the interpretation of the electromagnetic data. In the end, however, the indoor experiments may prove more useful for studying the effects of surface roughness since the indoor ice more nearly approached an idealized ice sheet.

V. Future Work

The experiments at CRREL suggested several future projects, both experimental and theoretical. One would be a surface scattering analysis for surface height distributions and correlation functions which were neither Gaussian nor exponential, but which were derived directly from experiment. Various groups have tried analytical forms for these functions other than the two mentioned above, but the physics behind why the roughness should follow one distribution rather than another is not clear, other than a simple

application of the central limit theorem leading to a Gaussian distribution. We would therefore like to attempt to include measured height distributions and correlation functions in scattering models. This would likely require numerical integration to calculate backscattering coefficients. Analysis of the most important features of the height distributions and correlation functions may tell us if and why simpler approximations such as a Gaussian form are realistic and physically correct.

A related theoretical problem has to do with the formation of roughness, both mechanical and dielectric. The snow-roughening experiments were appealing in that deposition of snow layers on ice is a natural process, more likely to occur than a sprinkling of ice particles. As mentioned in Section 3, however, the thick snow layer deposited on the indoor ice was hard to characterize, both in terms of the height variations and the dielectric constant variations due to brine wicked up into the snow. Outdoors, the thin snow layer deposited on the ice wicked up brine and hardened. In both cases, it would be of interest to know how the snow or slush layer changed in shape as it wicked up brine, and how the brine was distributed. Recent work[1] has shown that the rough interface that develops as fluid flows through some porous medium follows is self-affine and follows various scaling laws; it would be useful to extend this work to the systems of interest at CRREL, to include external forces such as evaporation and temperature changes, and to hopefully model the shape and brine distribution of a snow/slush layer on the ice as it forms.

Finally, an experimental problem that needs to be tackled is the devel-

opment of a better roughness gauge. We would like to maintain the unique features of our gauge – its ability to record the roughness of very thin, fragile ice surfaces and its bi-directional measuring method – while improving upon several aspects of it. One of these is the length: ideally we would like to have a gauge about a meter long, so that we can sample roughness that may be correlated over fairly long distances. To achieve this, we will have to solve problems of stability and rigidity. We would also like to design a gauge that could measure a two-dimensional roughness profile, rather than several linear transects. The desire for this became clear while measuring the roughness of the ice cube-roughened surface outdoors; visually the surface would appear quite rough, but linear transects would often only pick out a few height variations. How to achieve a two-dimensional profile is not yet clear. Finally, the gauge could be improved by having an electromagnetic height detection scheme rather than relying on photographs and hand digitization.

1. M. A. Rubio, C. A. Edwards, A. Dougherty, and J. P. Gollub, Phys. Rev. Lett. **63**, 1685 (1989); Y.-C. Zhang, J. Phys. (Paris) **51**, 2113 (1986); F. Family and T. Viscek, J. Phys. A **18**, L75 (1985). item

Table I

Preliminary roughness statistics for the indoor ice. Data are from hand traces of the long sides of the lightweight roughness gauge.

Date	*Location*	*State of Ice*	σ *(mm)* $\pm$ *0.2 mm*	*l (mm)* $\pm$?	*No. of samples averaged*
1/8/93	Near side	Unroughened	0.2	3.0	4
1/9/93	Near side	Unroughened	0.2	5.0	16
1/10/93	Near side	Unroughened	0.2	10.0	2
1/11/93	Near side	Unroughened	0.3	6.0	4
1/13/93	Near side	Unroughened	0.5	5.0	12
1/13/93	Far side	Unroughened	0.4	5.0	10
1/14/93	Far side	Unroughened	0.5	12.0	2
1/15/93	Near side	Unroughened	0.4	7.0	4
1/15/93	Far side	Ice cubes, before spray	3.0	7.0	6
1/16/93	Far side	Ice cubes, after 1st spray	3.0	6.0	8
1/16/93	Far side	Ice cubes, after 2nd spray	2.0	8.0	8

FIGURE CAPTIONS

1. Lightweight surface roughness gauge.
2. String of several metal, 6-inch roughness gauges.
3. Large roughness gauge; rods spaced 1 cm apart.
4. Sample of roughness statistics generated in real time at CRREL; clockwise from top left: height profile, height distribution function, correlation function, fit to correlation function.
5. Far side of indoor ice, where pancake ice formed initially.
6. Near side of indoor ice.
7. Indoor ice thickness vs. time.
8. Snow layer deposited on indoor ice surface.
9. Part of snow layer deposited on indoor ice surface.
10. Ice cube layer deposited on indoor ice surface, after first spraying.
11. Ice cube layer deposited on indoor ice surface, after second spraying.
12. Ice on outdoor pond in unroughened state (1/19/93).
13. Pond ice thickness vs. time.
14. Outdoor pond ice with part of surface covered with thin snow layer; remainder of surface left in natural state.

15. Snow-roughened part of pond ice surface.

16. Outdoor pond ice with part of surface covered with crushed ice cubes; remainder of surface left in natural state.

17. Ice cube-roughened part of pond ice surface.

18. Salinity vs. depth for 2.7 cm thick slab of indoor ice.

19. Salinity vs. depth for 4.35 cm thick slab of indoor ice.

20. Salinity vs. depth for 7.5 cm thick slab of indoor ice.

21. Salinity vs. depth for 9.5 cm thick slab of indoor ice.

22. 9 salinity scrapings from snow layer deposited on the indoor ice surface.

23. 11 salinity scraping from snow layer deposited on the indoor ice surface.

24. Frost flowers on the far side of the indoor pit.

25. Near surface salinities of outdoor ice from 1/28/93.

26. Near surface salinities of outdoor ice from 1/29/93, morning and afternoon.

27. Near surface salinities of outdoor ice from 1/29/93, night.

28. Salinity vs. depth of 2 pond ice samples: 1/27 is unroughened, 1/30 is snow-roughened.

29. Roughness statistics from a measurement of the ice cube-roughened indoor ice, after the 2nd spraying. Note the bimodal height distribution.

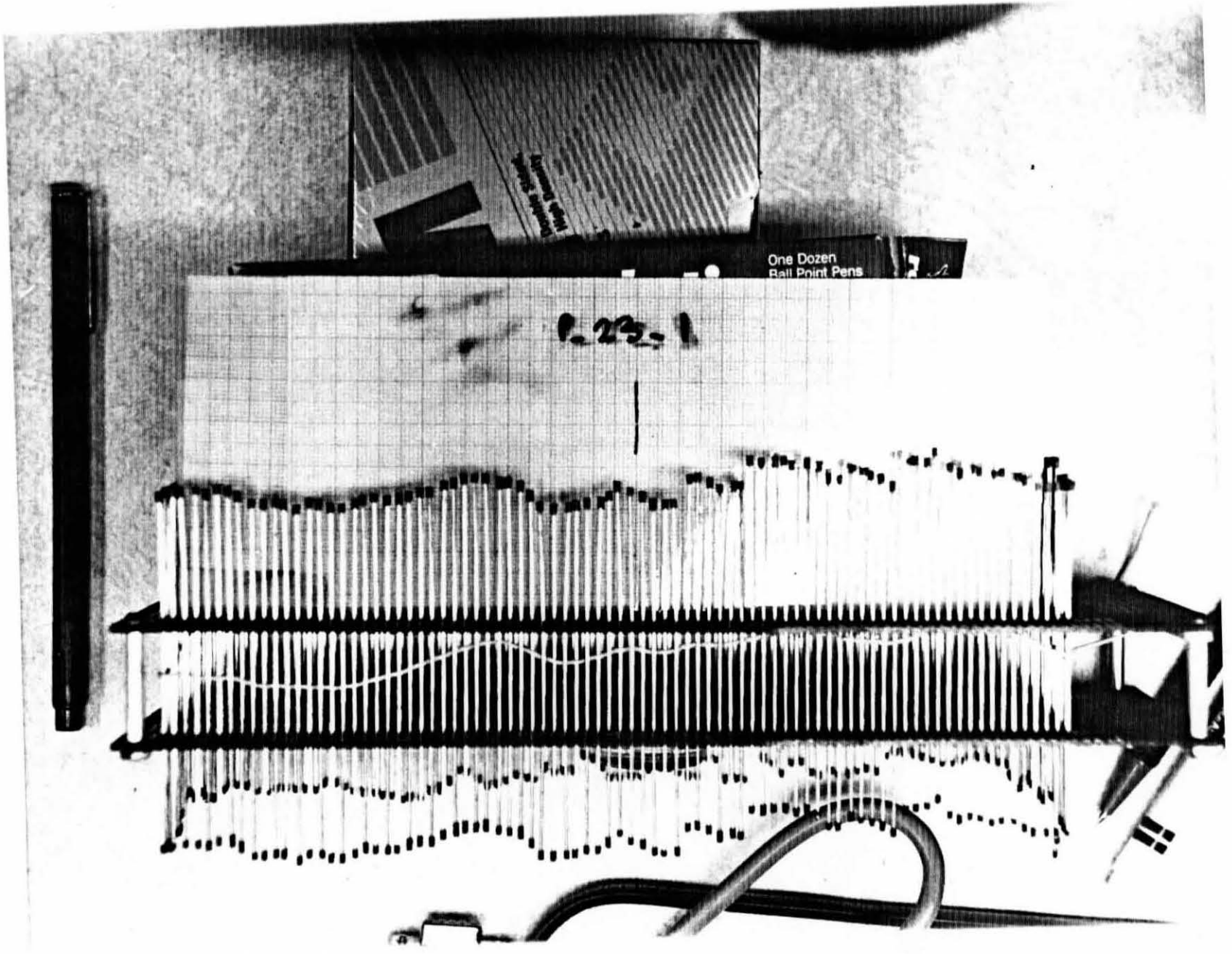

Figure 1

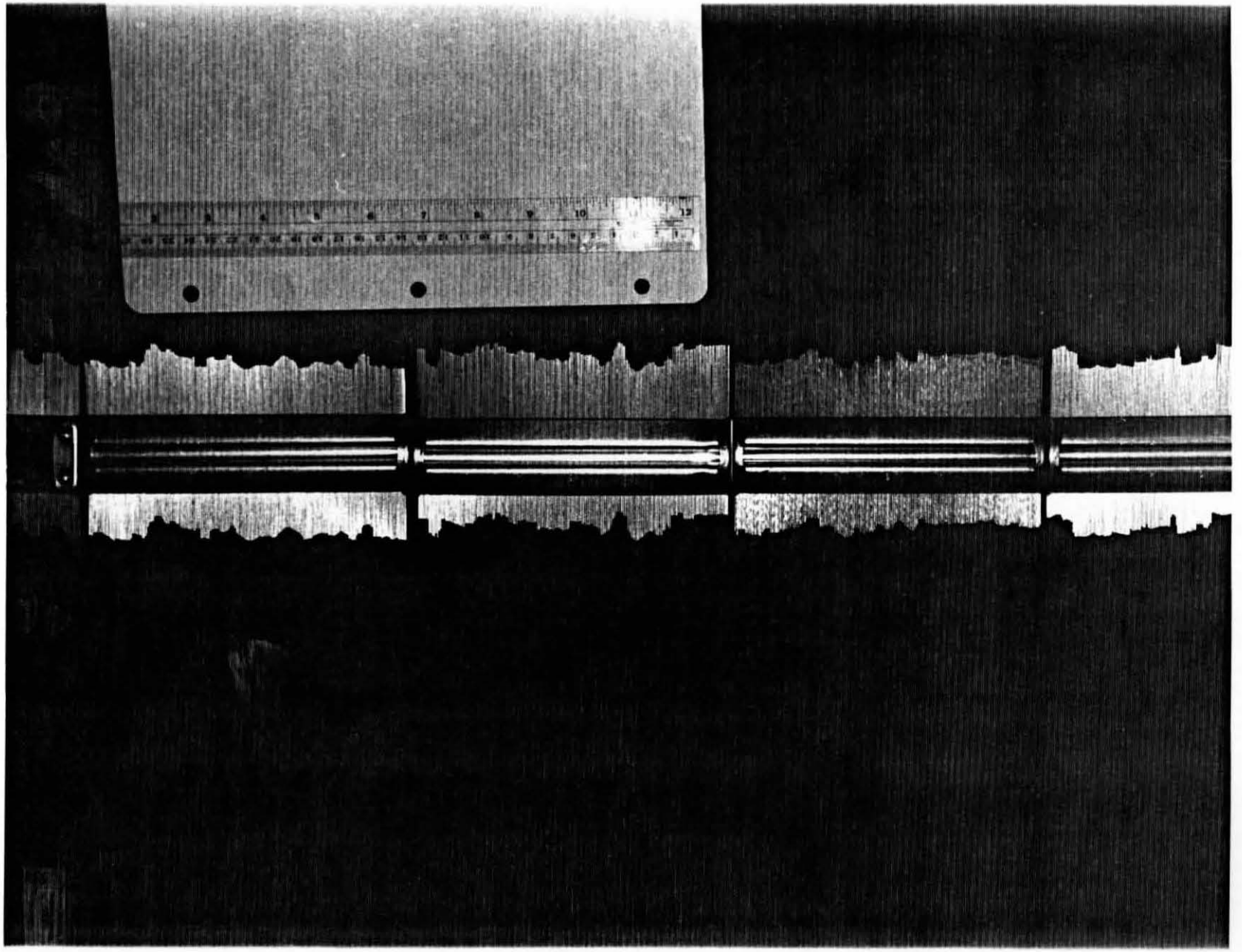

Figure 2

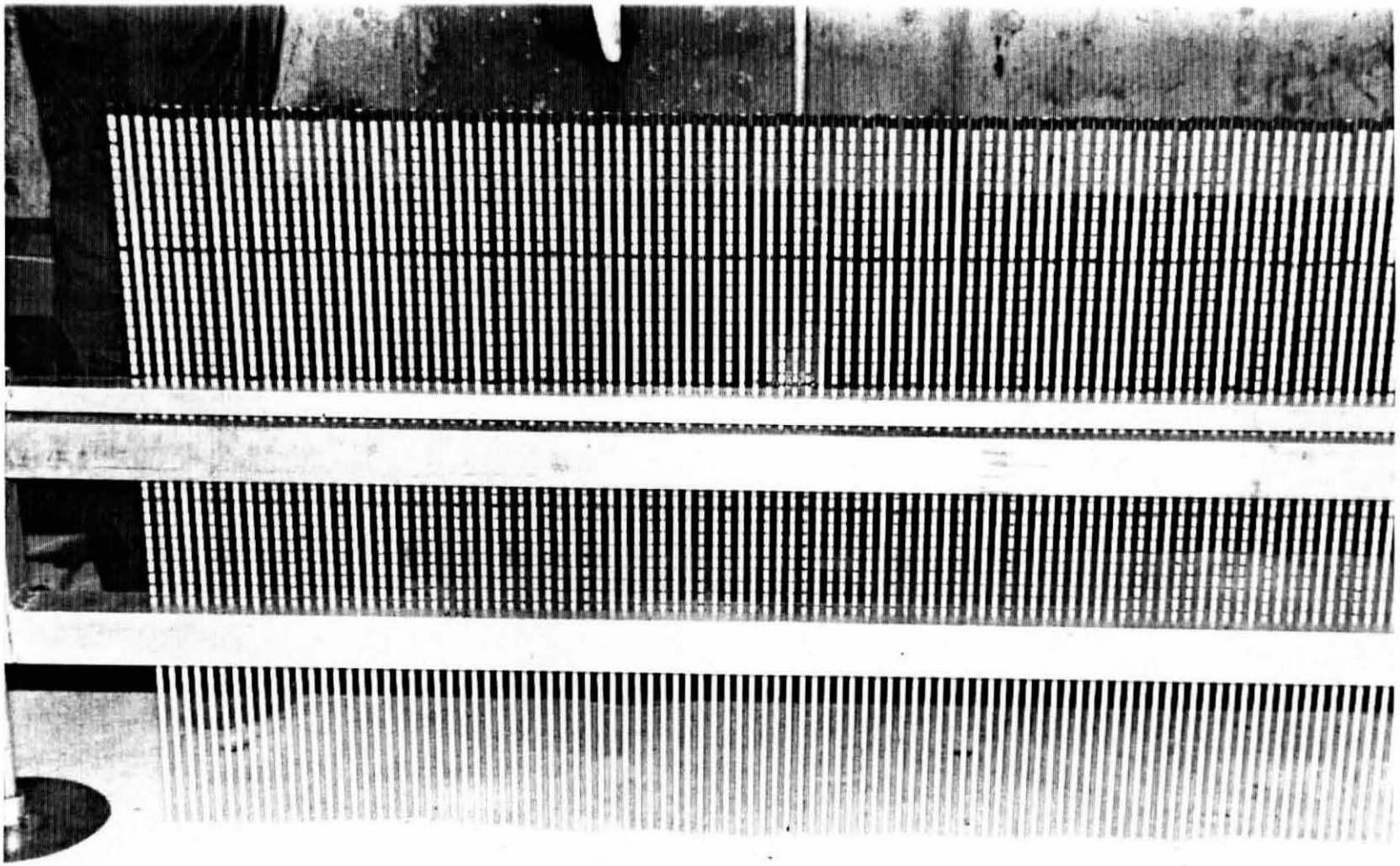

Figure 3

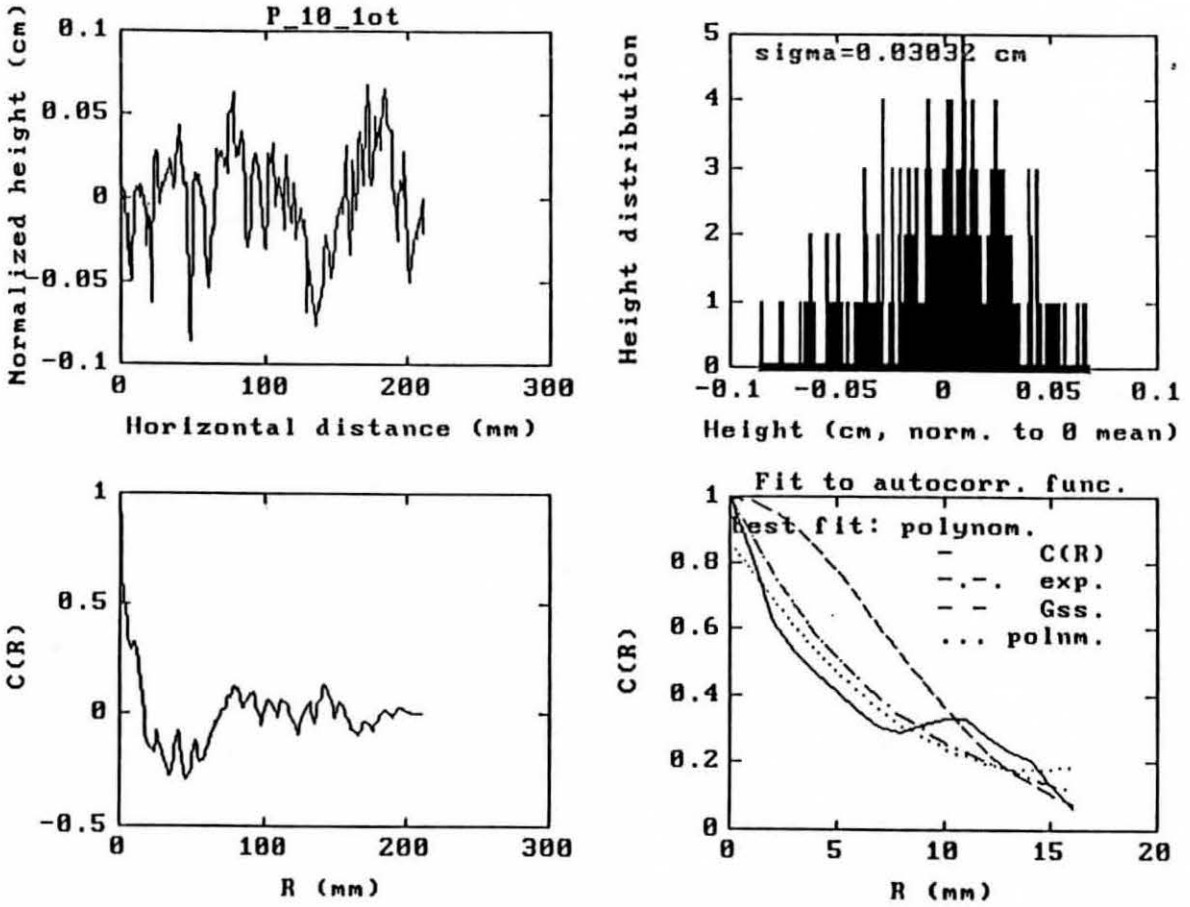

Near side of indoor ice, unroughened (1/11/93)

Figure 4

Figure 5

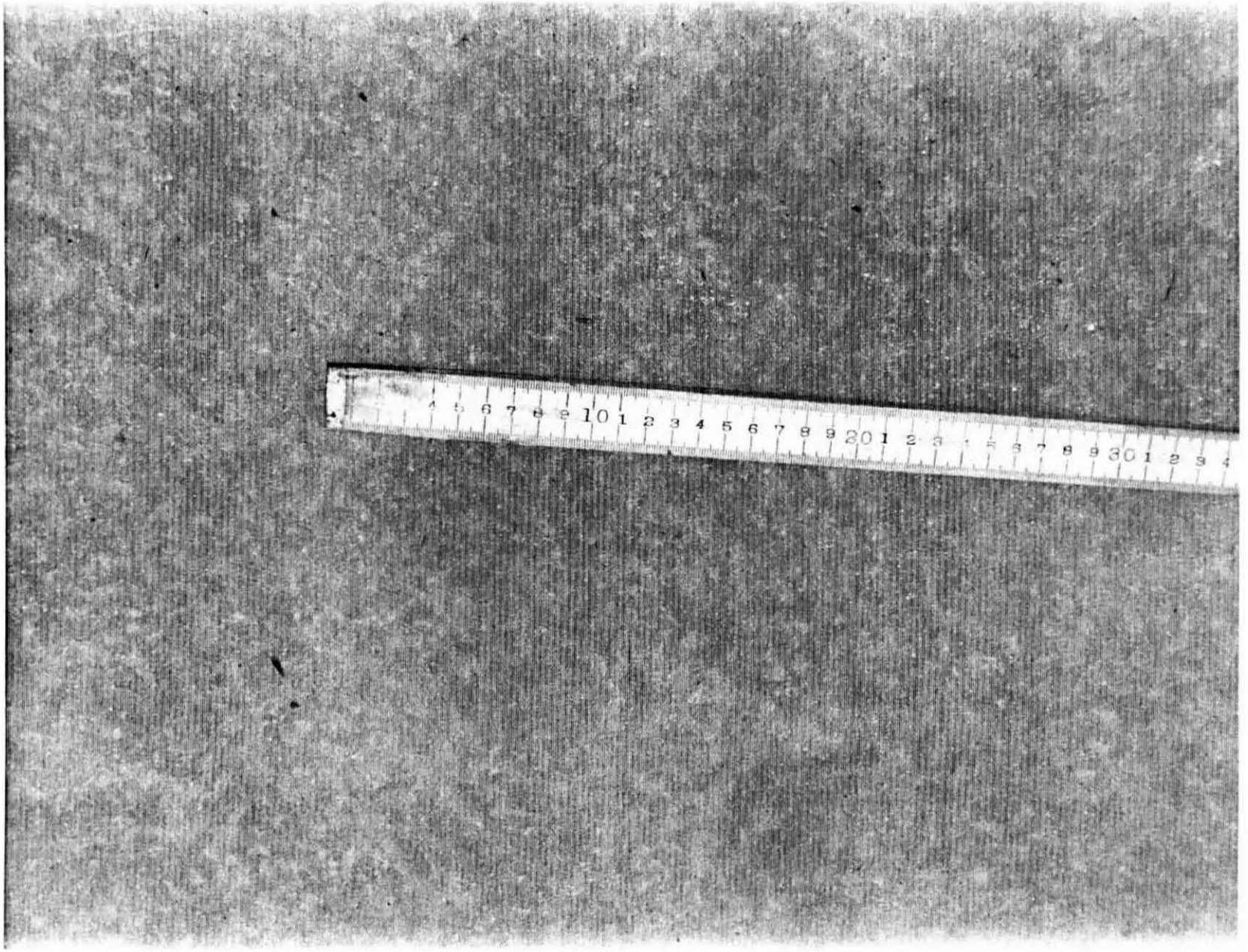

Figure 6

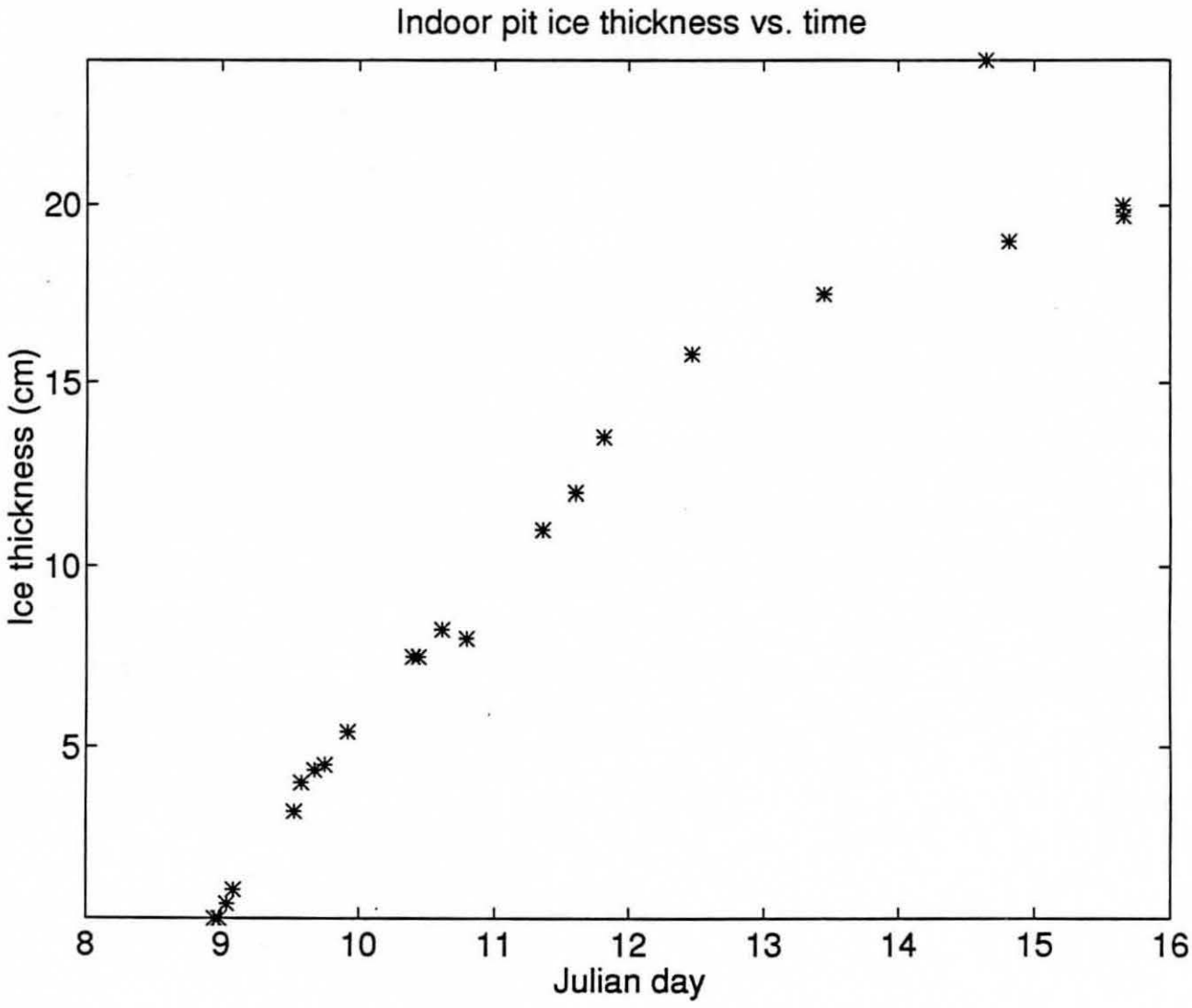
Indoor pit ice thickness vs. time
Ice thickness (cm)
Julian day
5
10
15
20
8
9
10
11
12
13
14
15
16

Figure 7

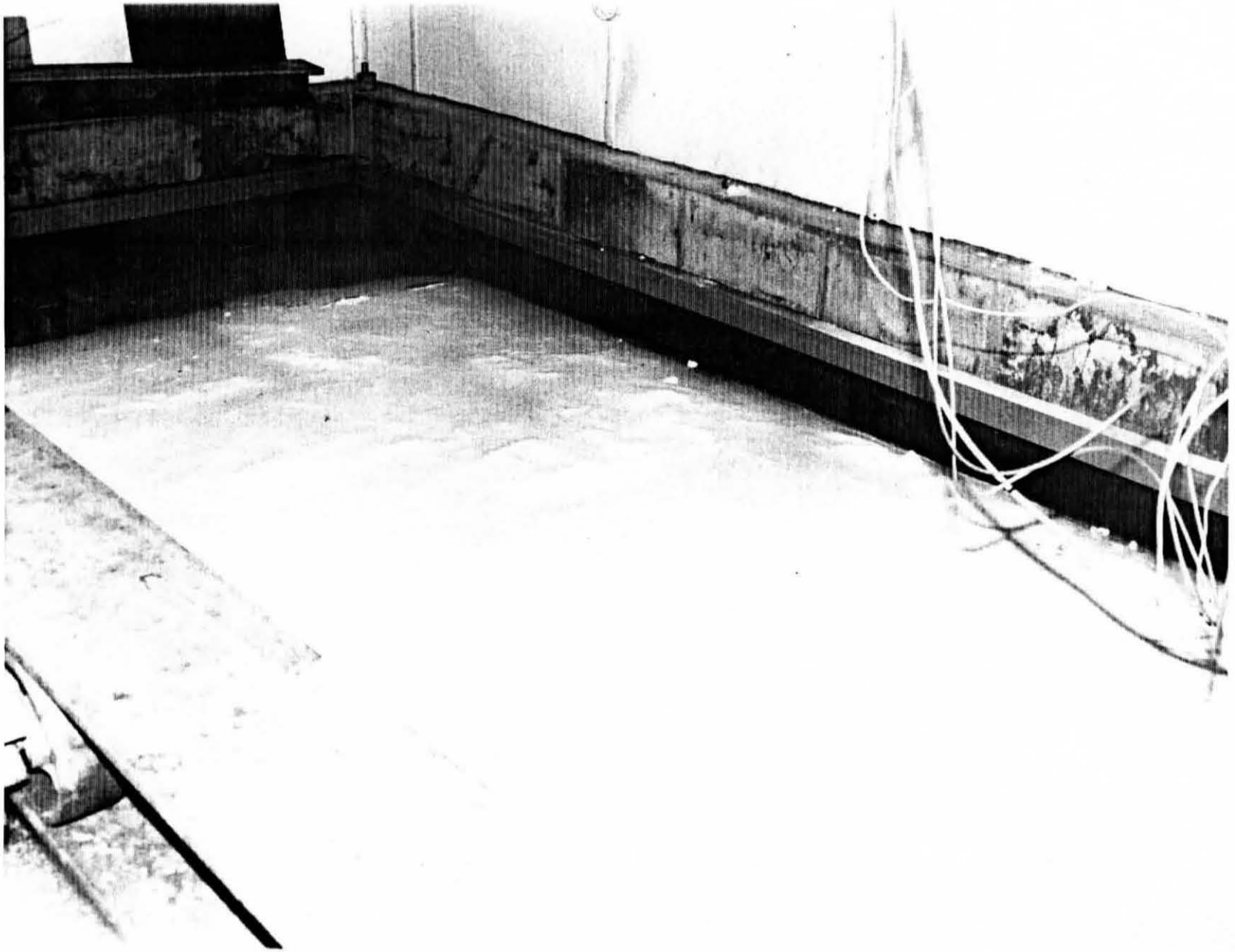

Figure 8

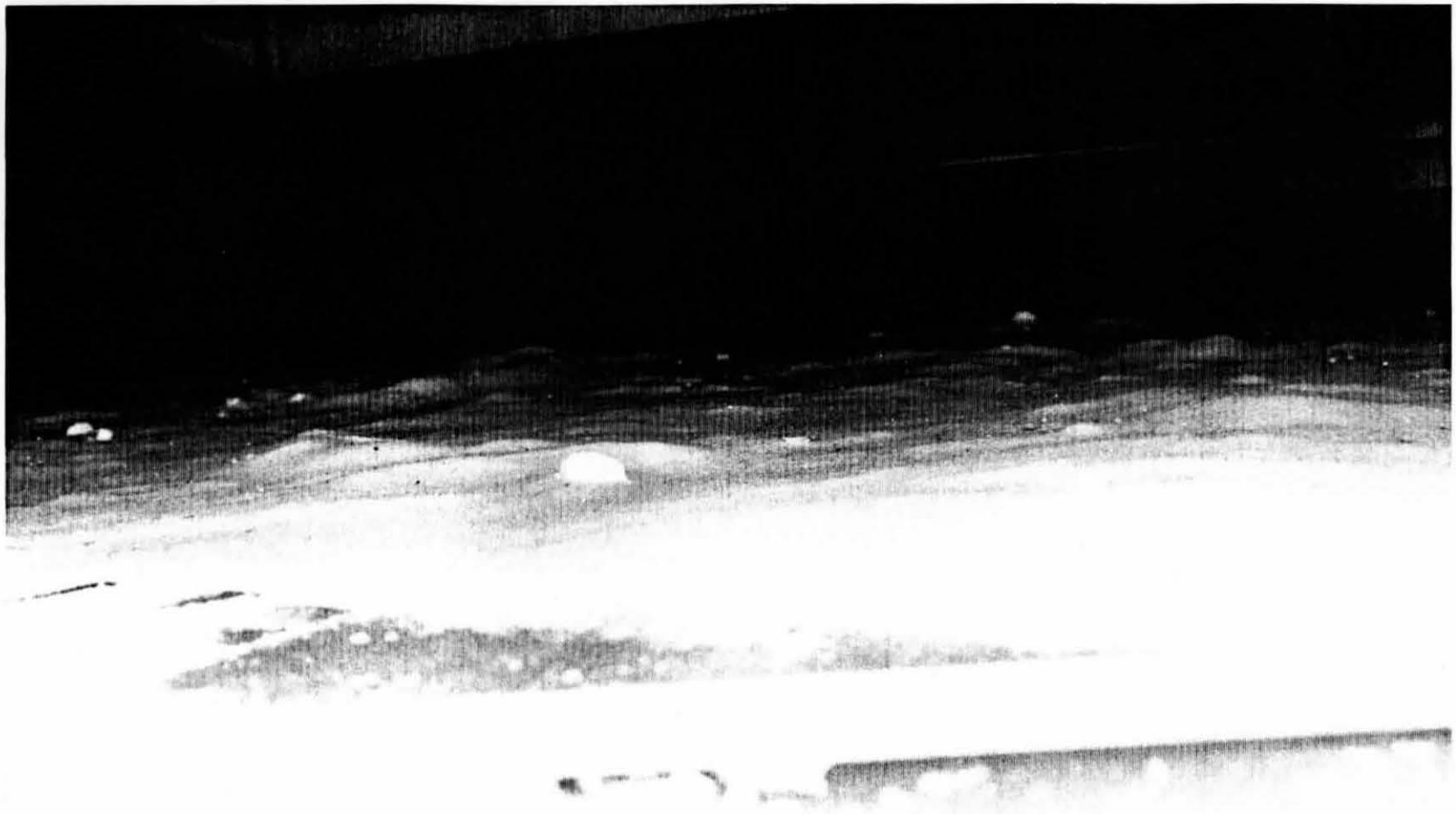

Figure 9

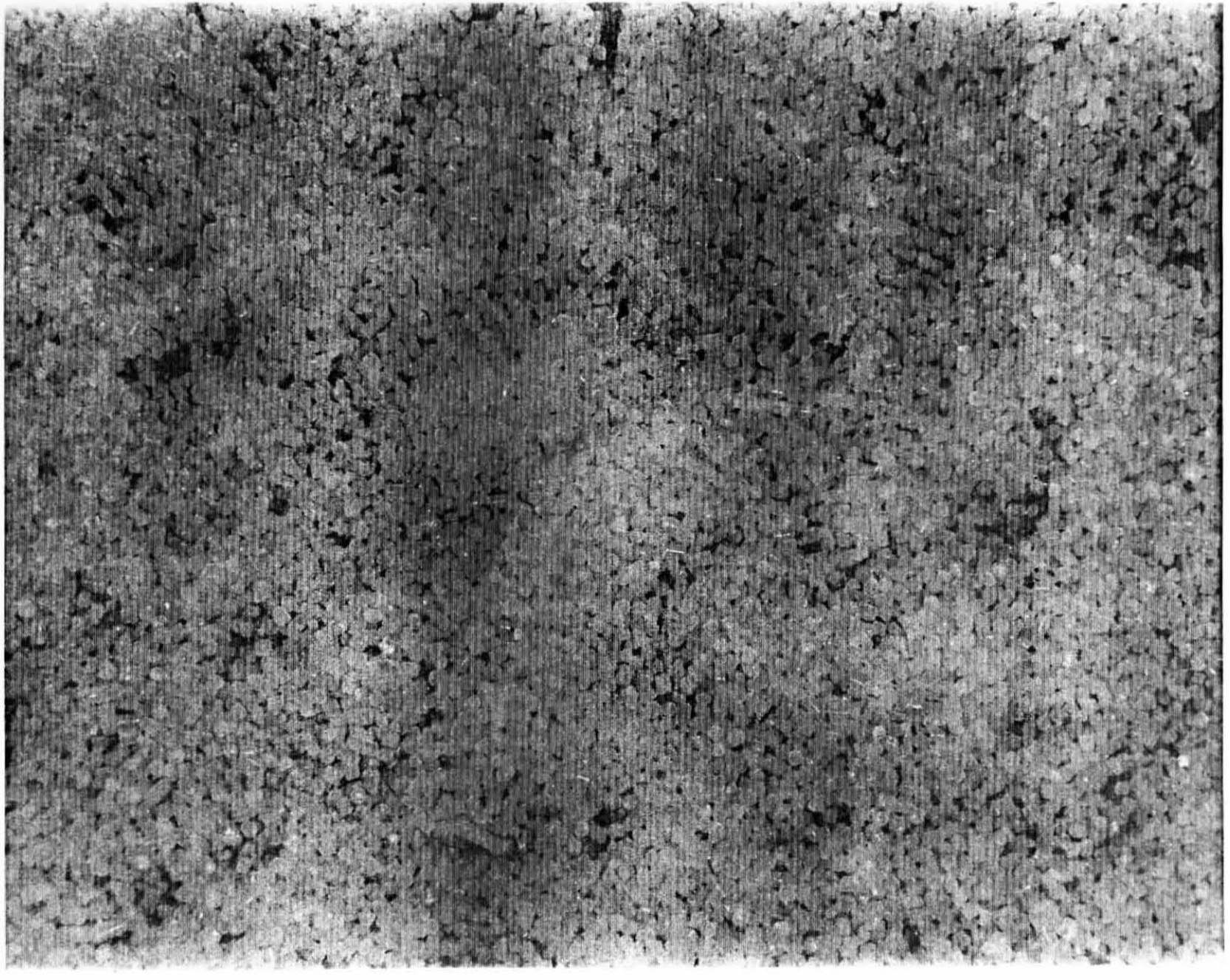

Figure 10

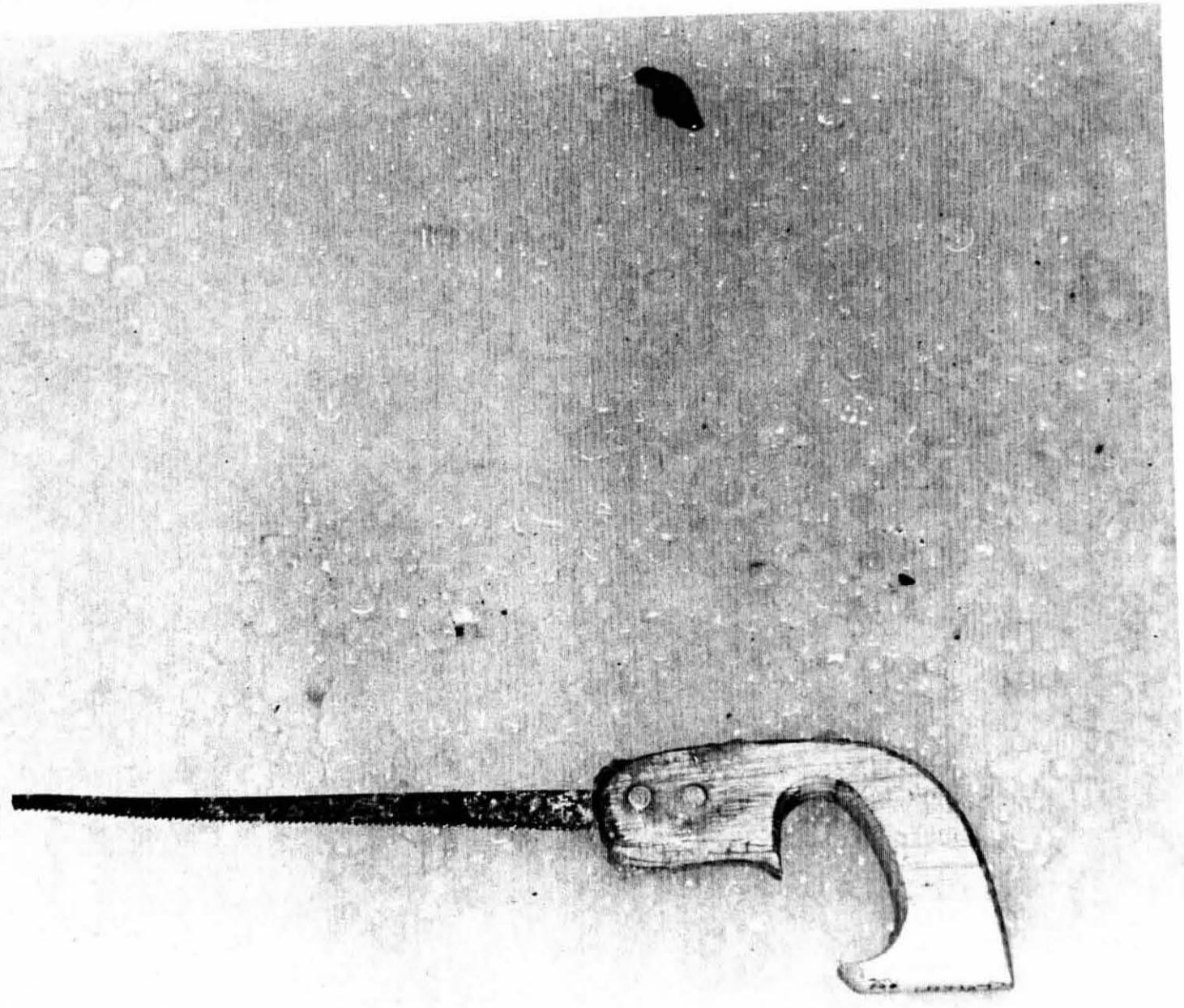

Figure 11

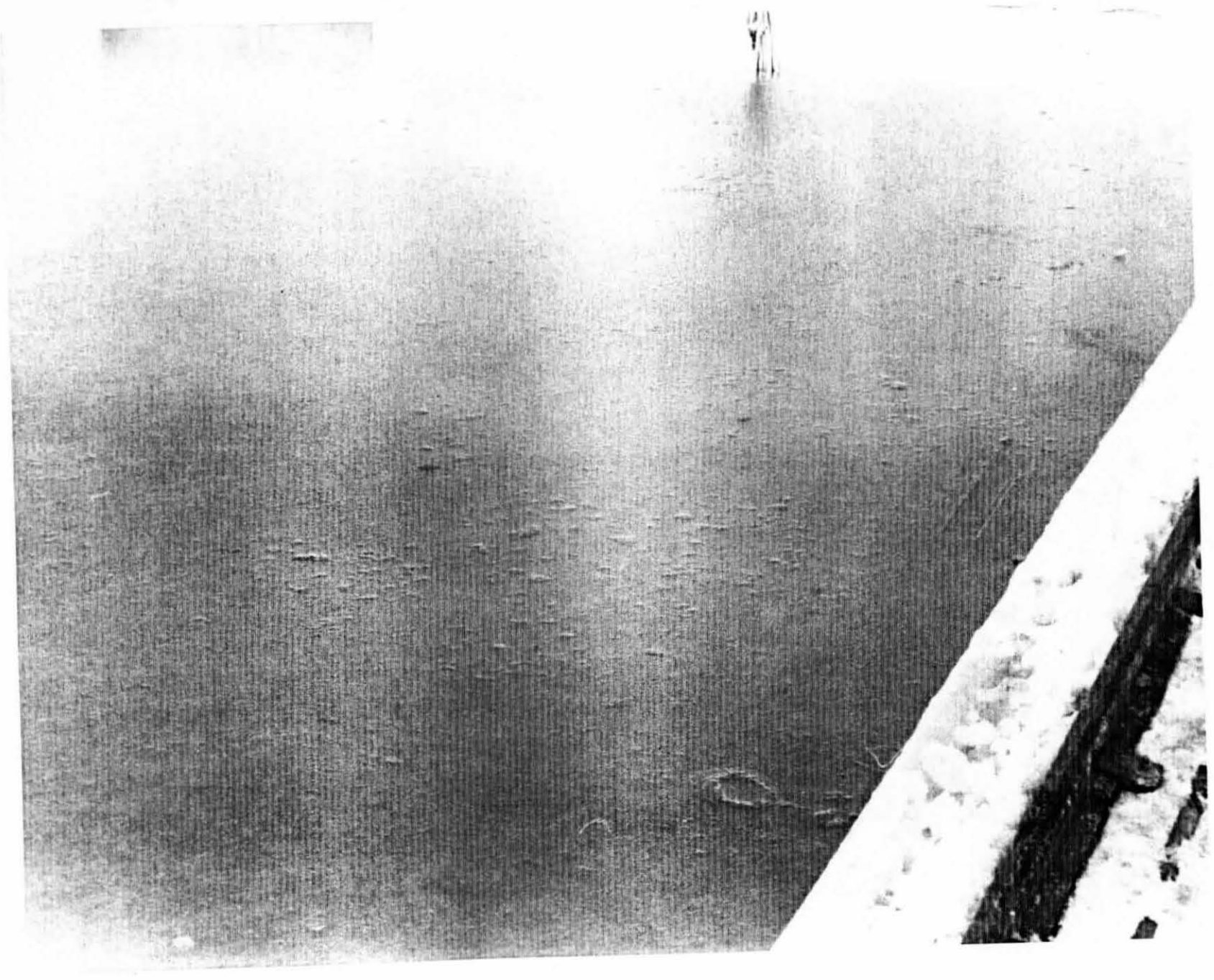

Figure 12

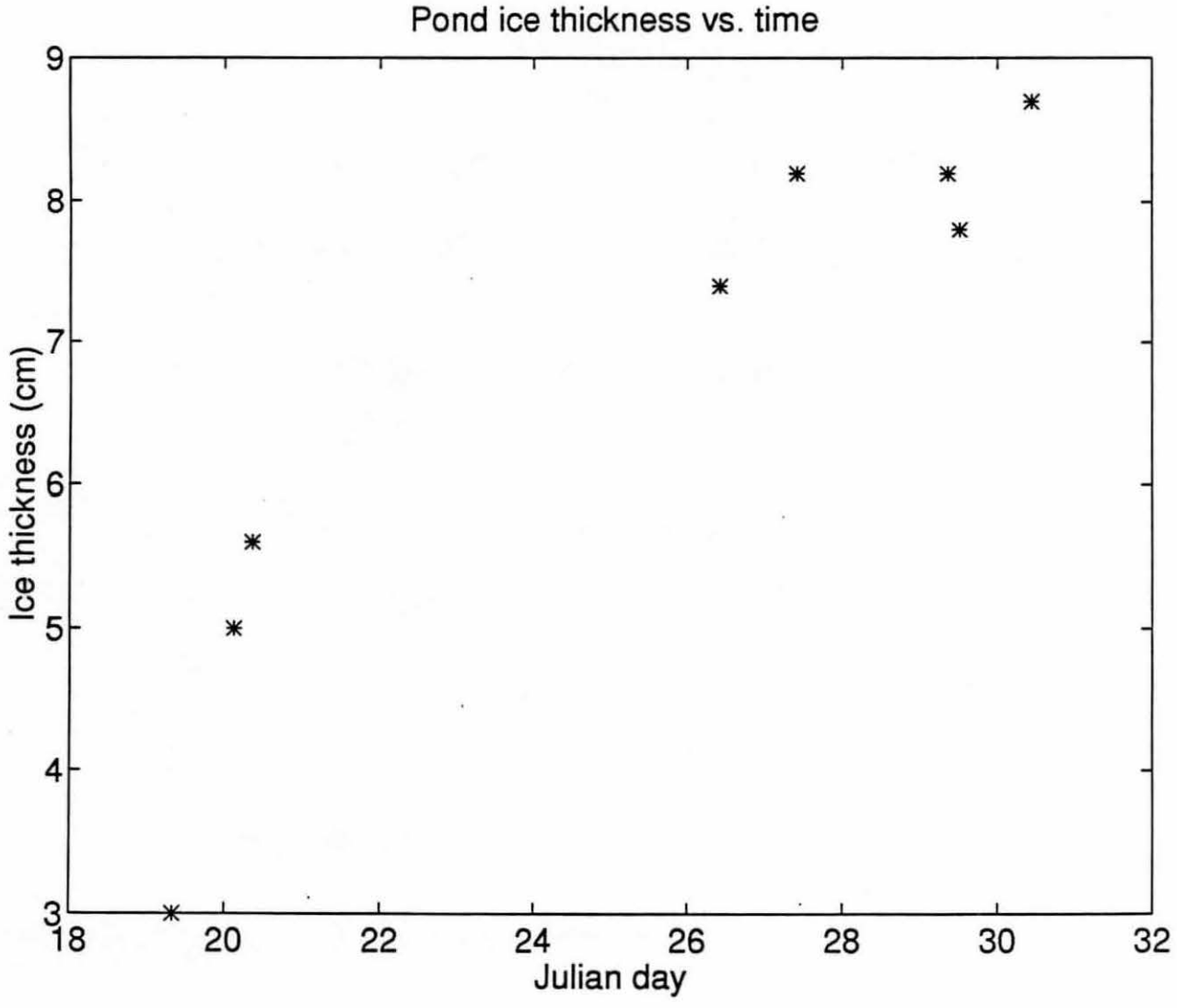
Pond ice thickness vs. time
Ice thickness (cm)
Julian day
9
8
7
6
5
4
3
18
20
22
24
26
28
30
32

Figure 13

Figure 14

Figure 15

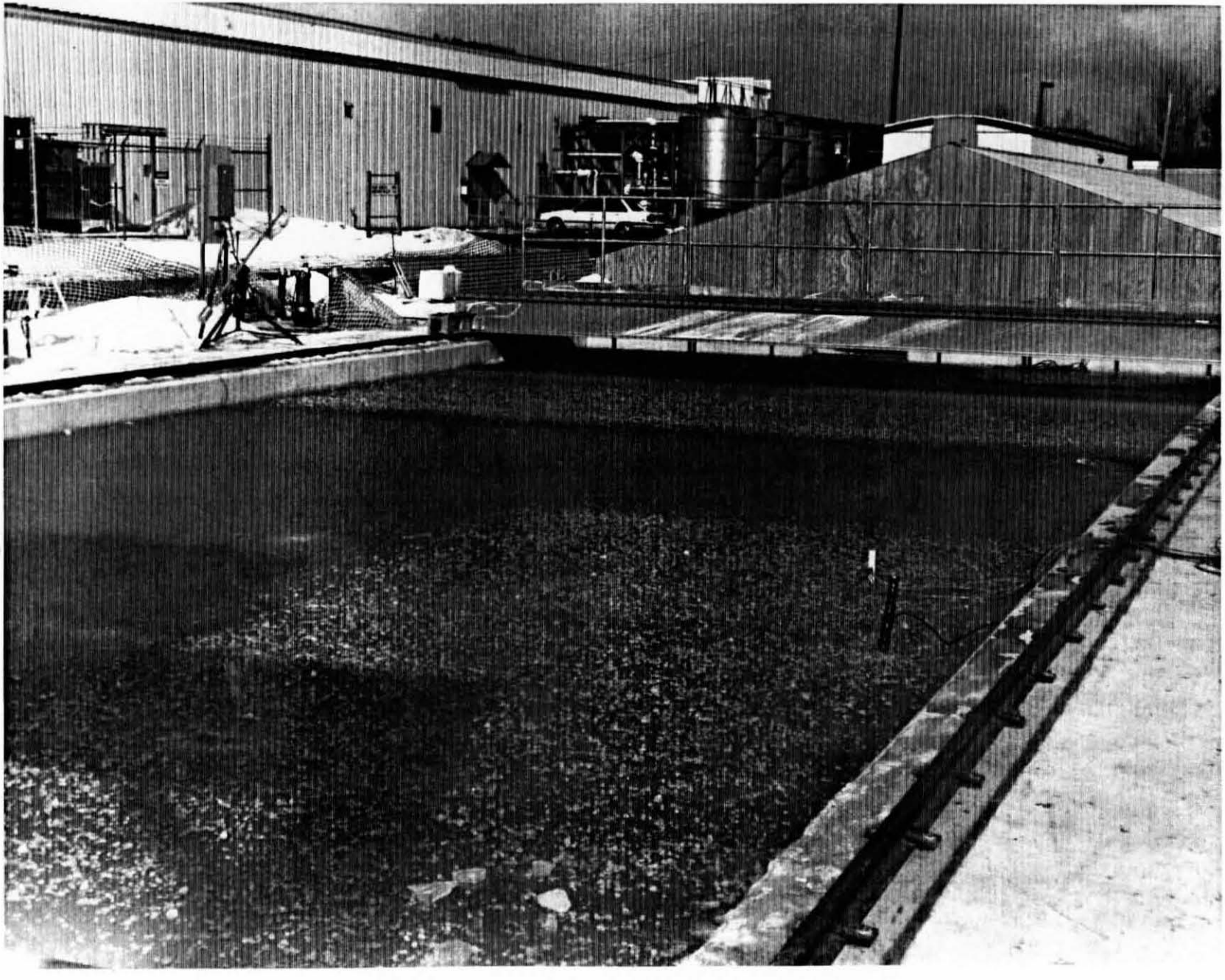

Figure 16

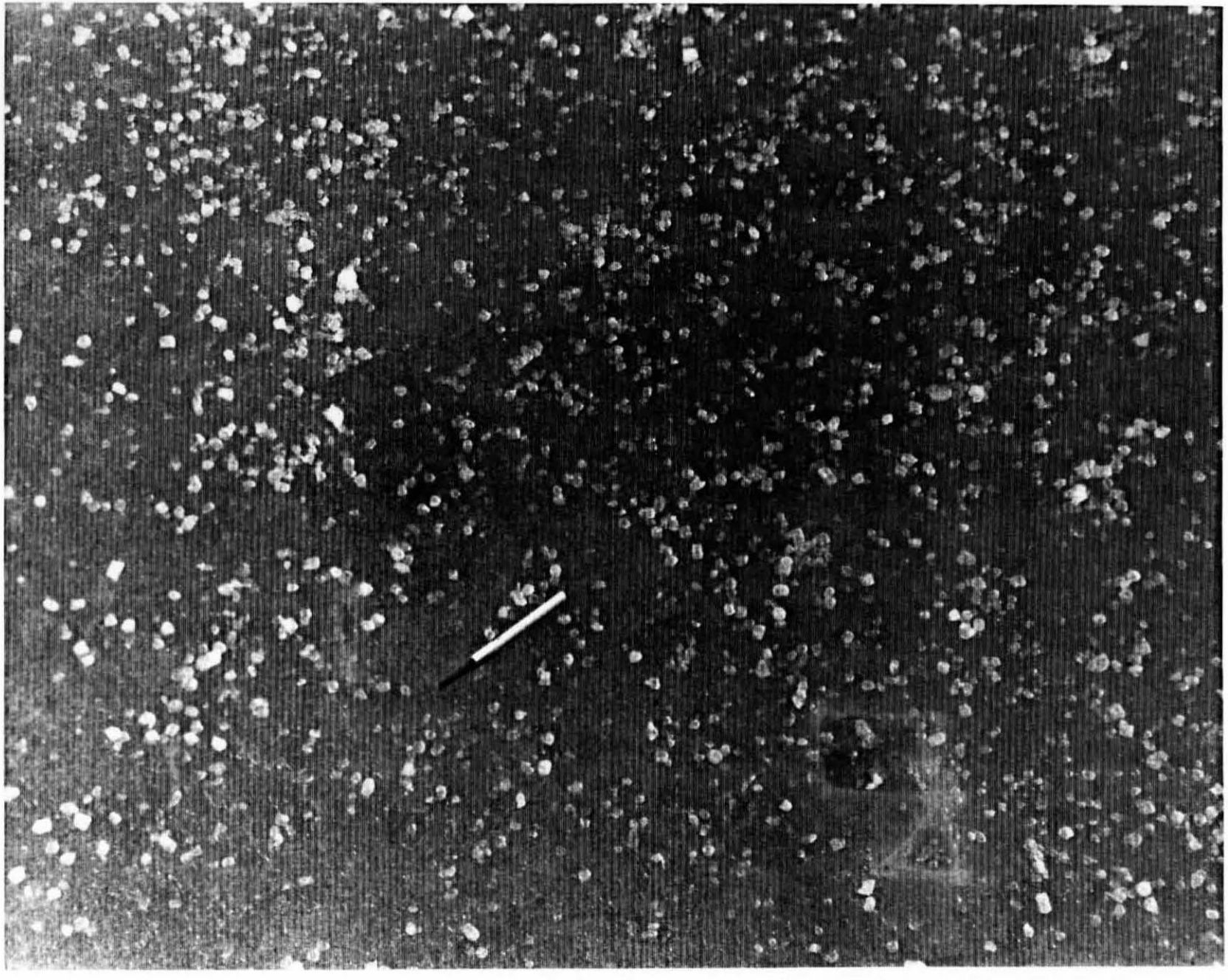

Figure 17

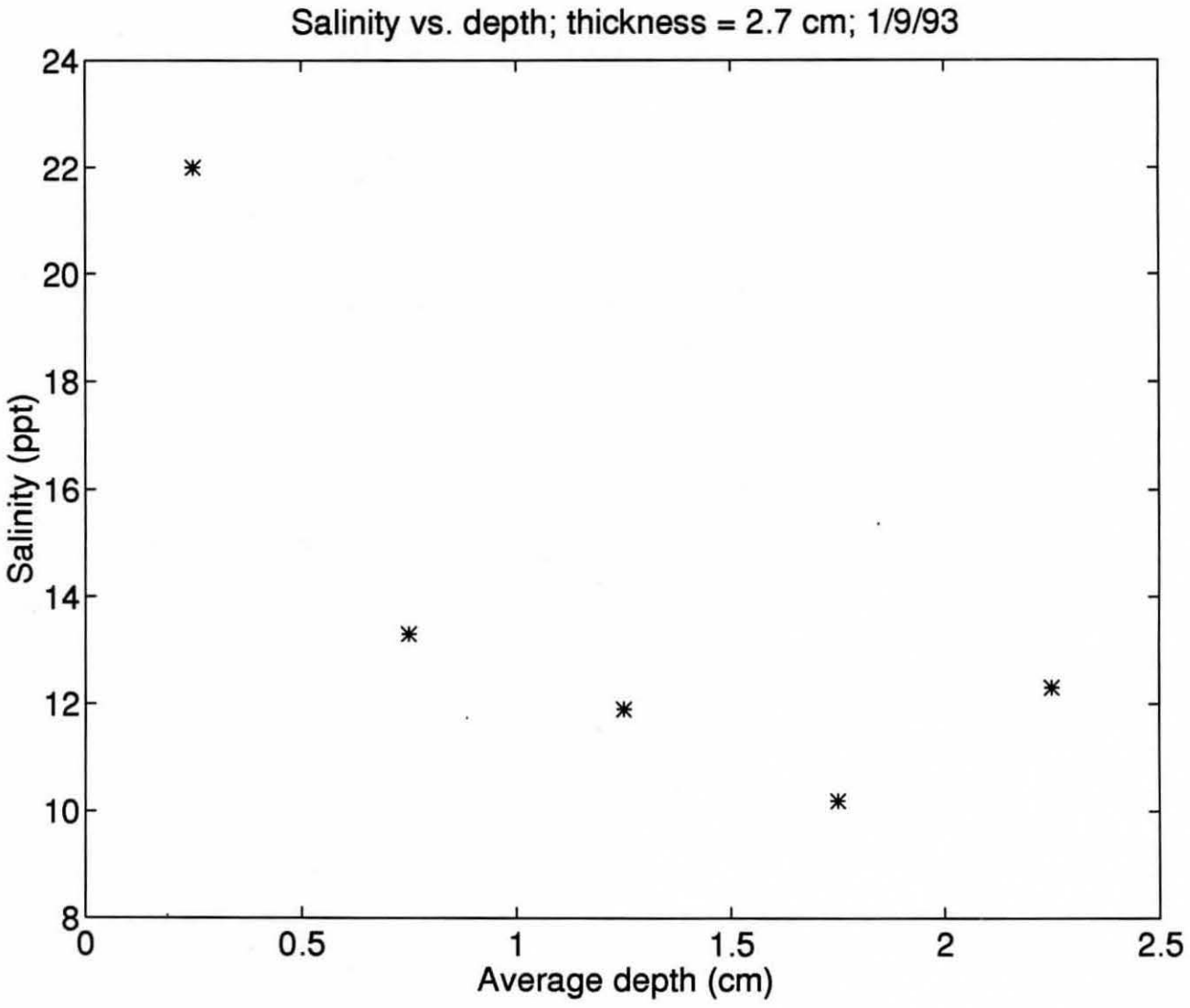
Salinity vs. depth; thickness = 2.7 cm; 1/9/93
Salinity (ppt)
Average depth (cm)
24
22
20
18
16
14
12
10
8
0
0.5
1
1.5
2
2.5

Figure 18

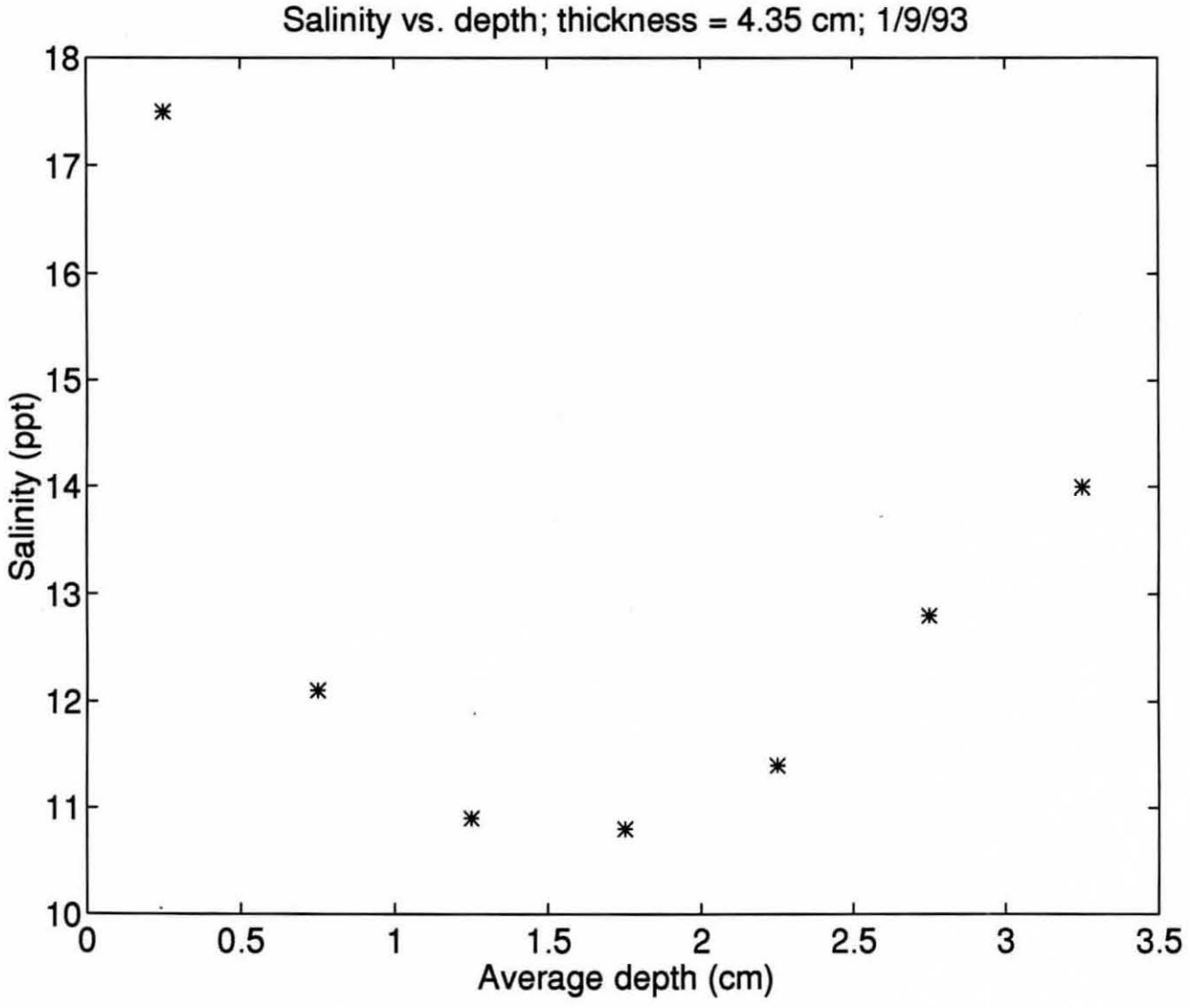
Salinity vs. depth; thickness = 4.35 cm; 1/9/93
Salinity (ppt)
Average depth (cm)
18
17
16
15
14
13
12
11
10
0
0.5
1
1.5
2
2.5
3
3.5

Figure 19

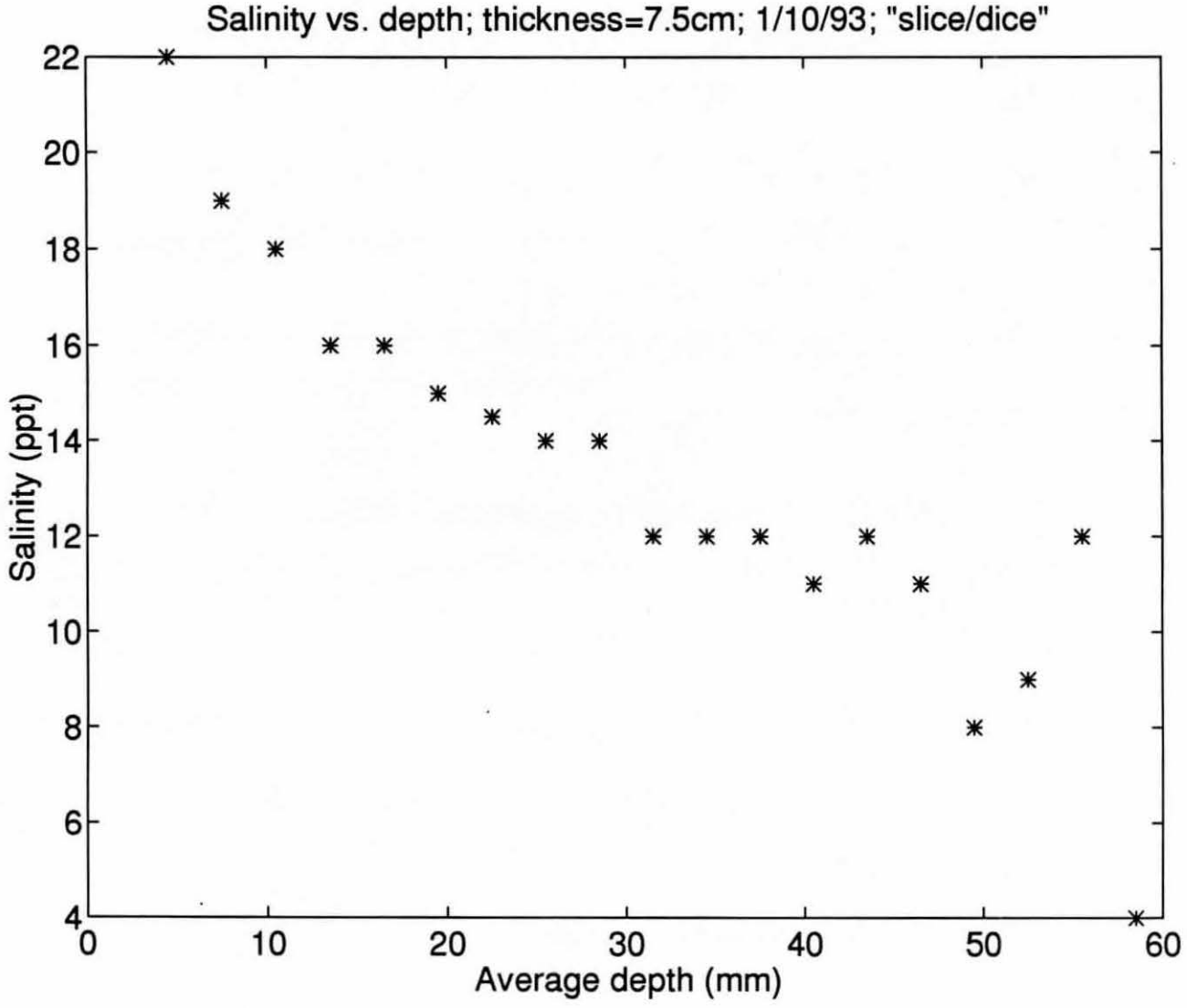
Salinity vs. depth; thickness=7.5cm; 1/10/93; "slice/dice"
Salinity (ppt)
Average depth (mm)
22
20
18
16
14
12
10
8
6
4
0
10
20
30
40
50
60

Figure 20

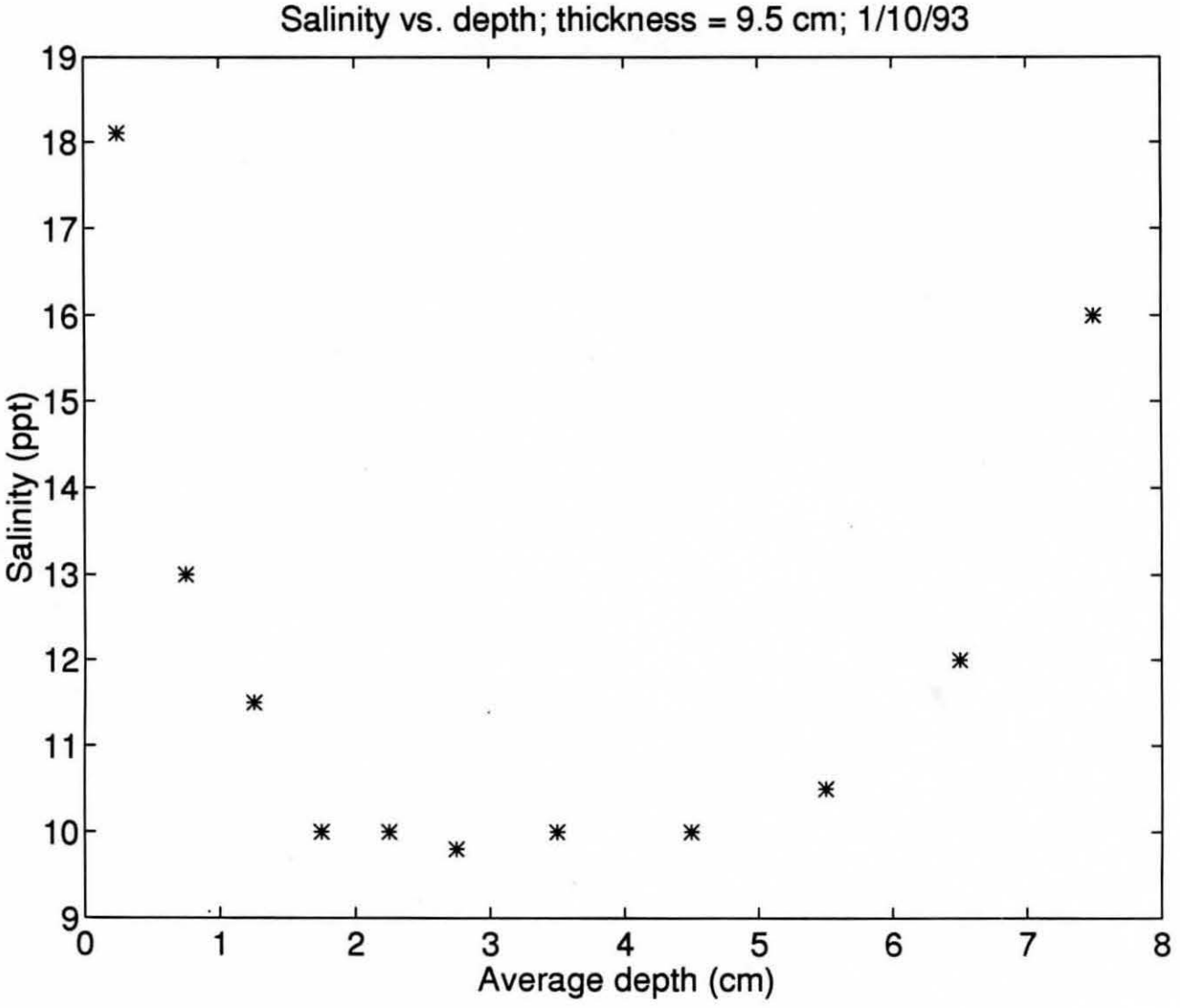
Salinity vs. depth; thickness = 9.5 cm; 1/10/93
Salinity (ppt)
Average depth (cm)
19
18
17
16
15
14
13
12
11
10
9
0
1
2
3
4
5
6
7
8

Figure 21

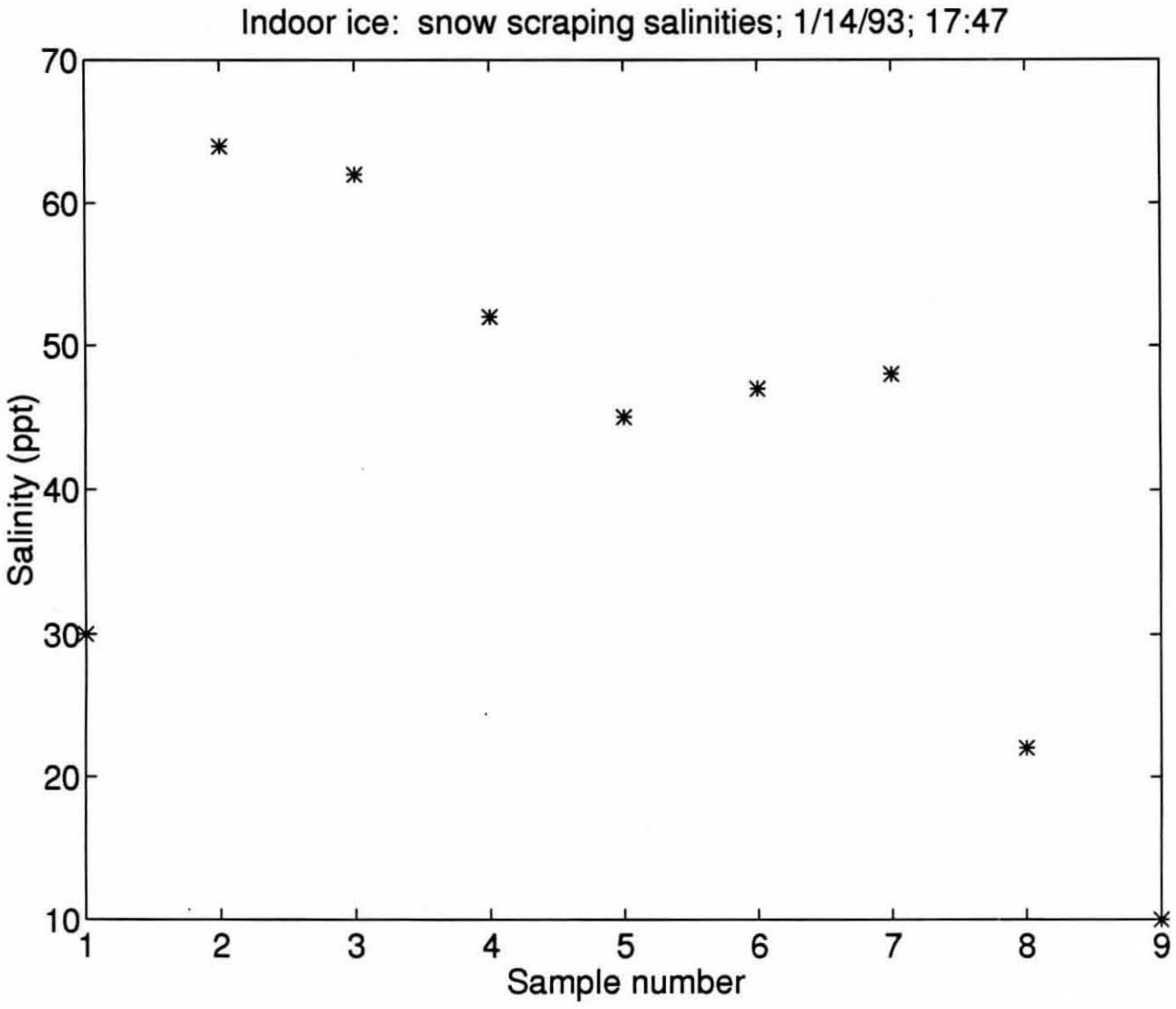
Indoor ice: snow scraping salinities; 1/14/93; 17:47
Salinity (ppt)
70
60
50
40
30
20
10
1
2
3
4
5
6
7
8
9
Sample number

Figure 22

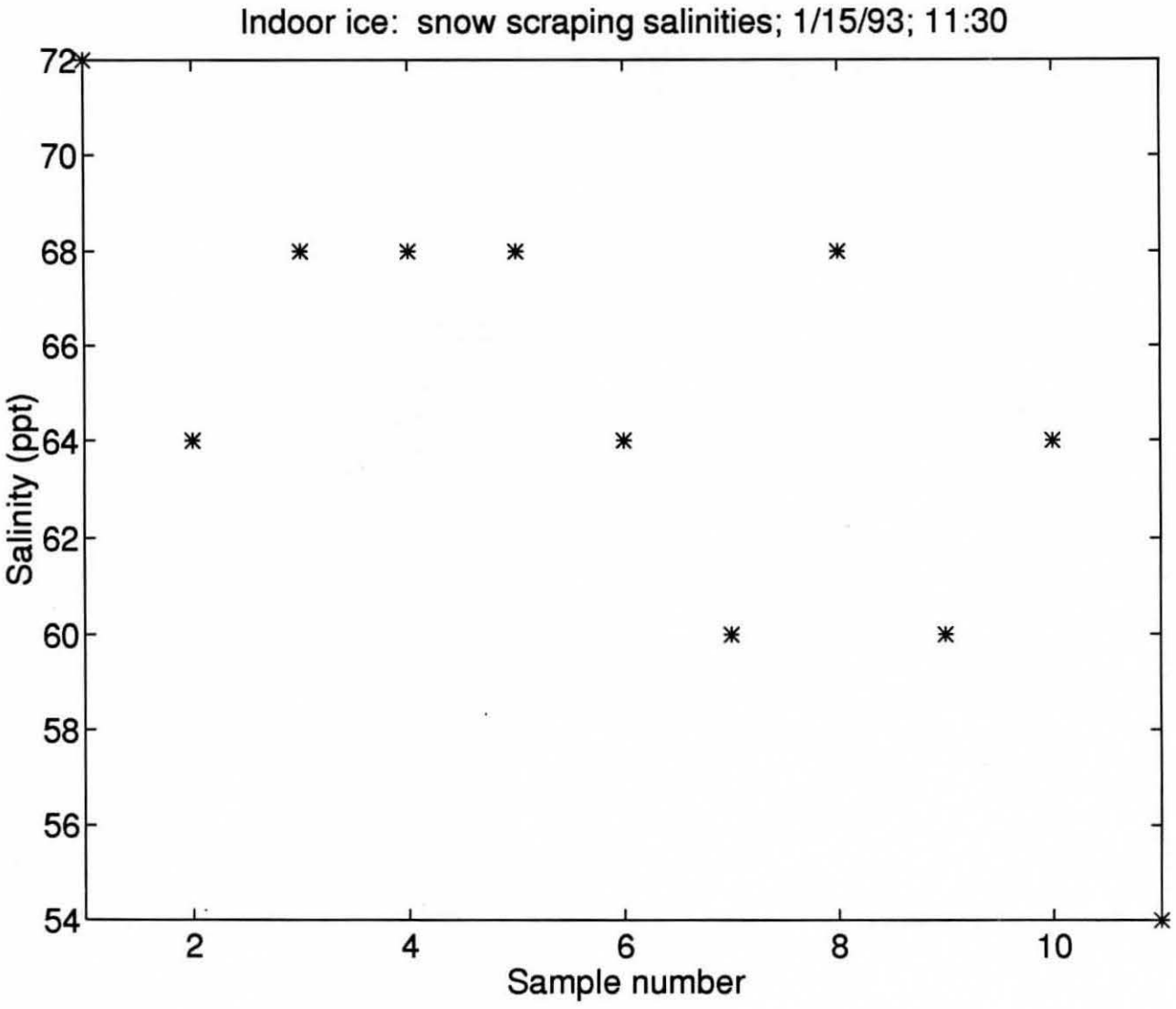
Indoor ice: snow scraping salinities; 1/15/93; 11:30
Salinity (ppt)
72
70
68
66
64
62
60
58
56
54
2
4
6
8
10
Sample number

Figure 23

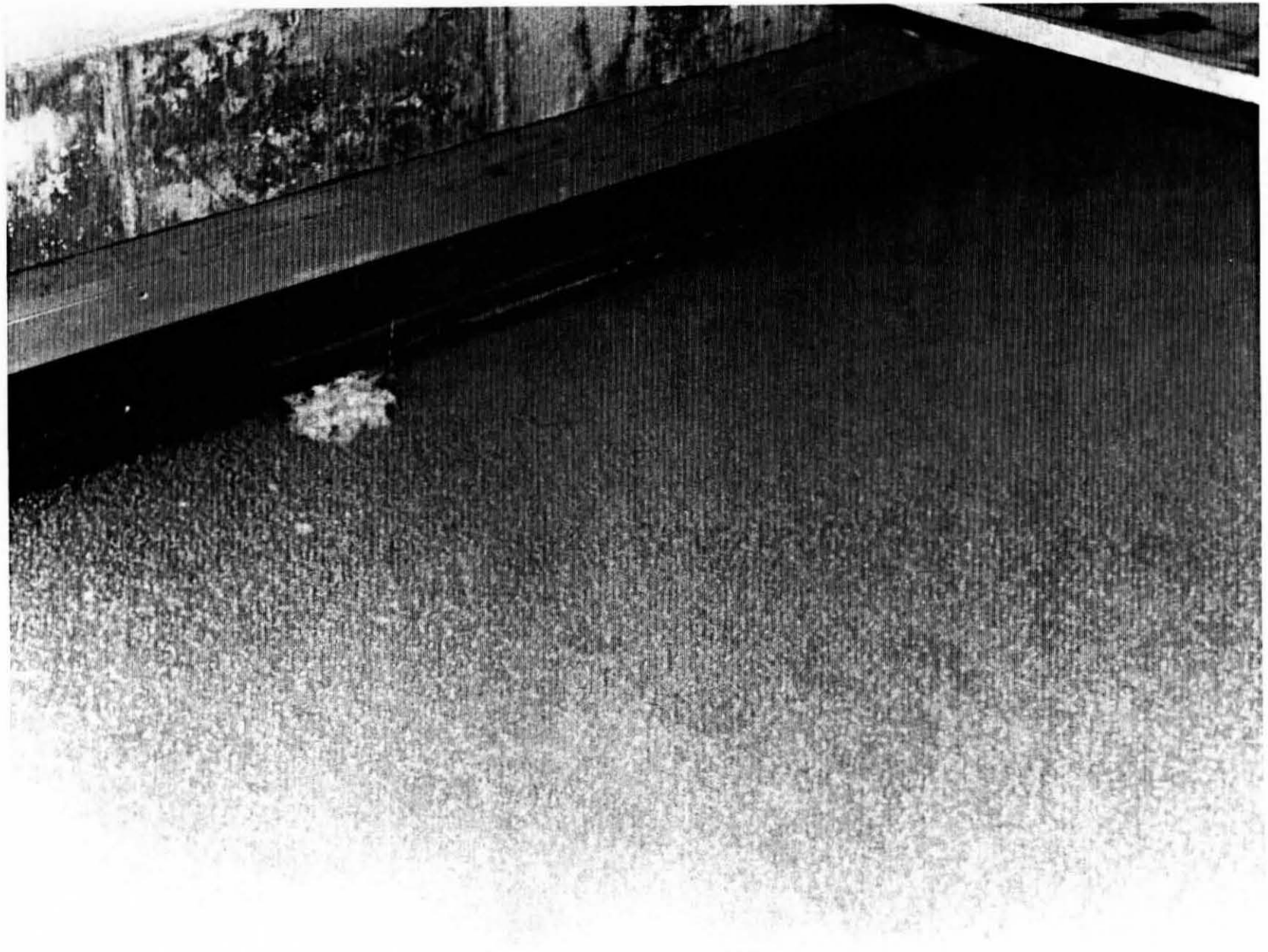

Figure 24

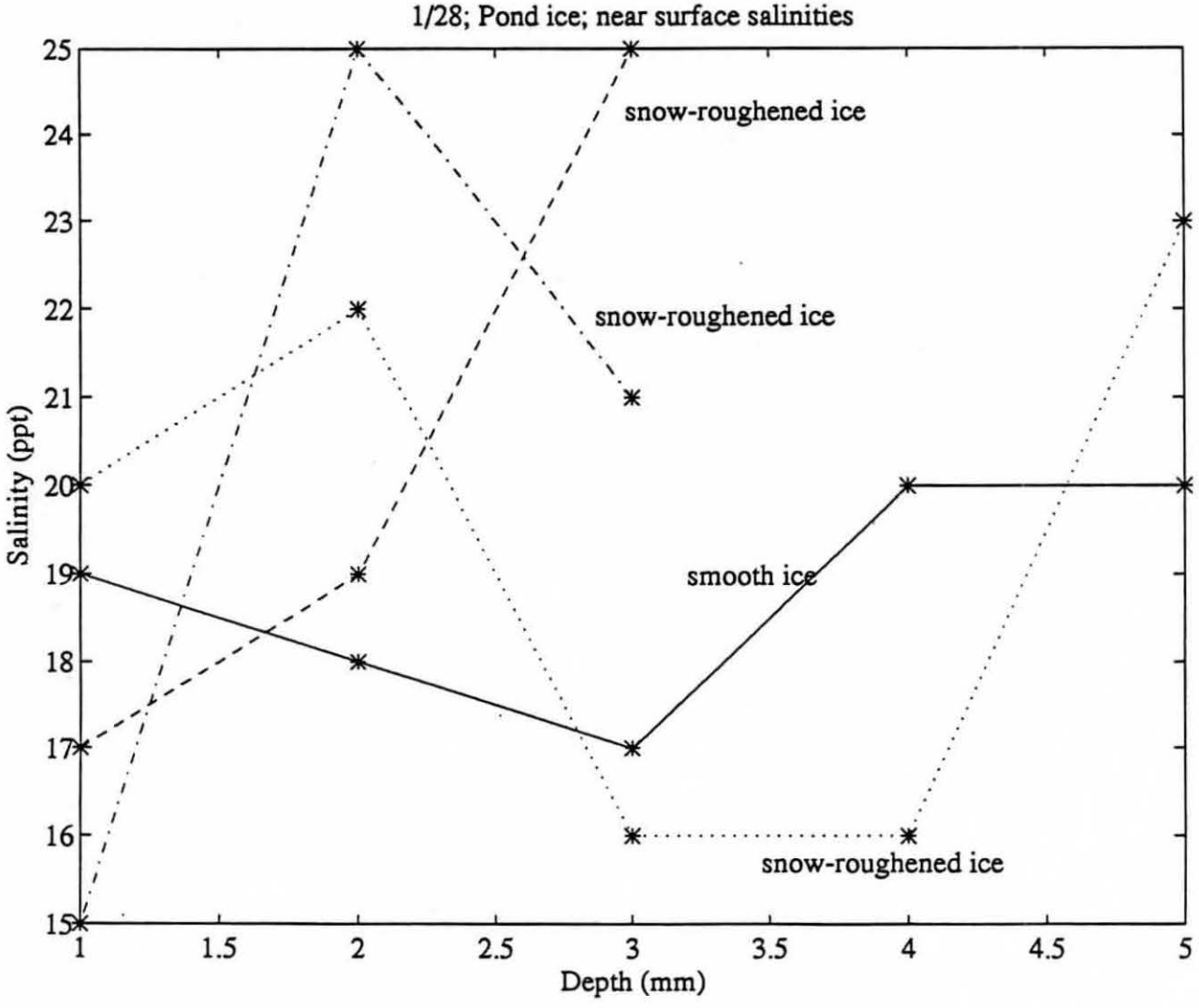
1/28; Pond ice; near surface salinities
Salinity (ppt)
Depth (mm)
snow-roughened ice
snow-roughened ice
smooth ice
snow-roughened ice
25
24
23
22
21
20
19
18
17
16
15
1
1.5
2
2.5
3
3.5
4
4.5
5

Figure 25

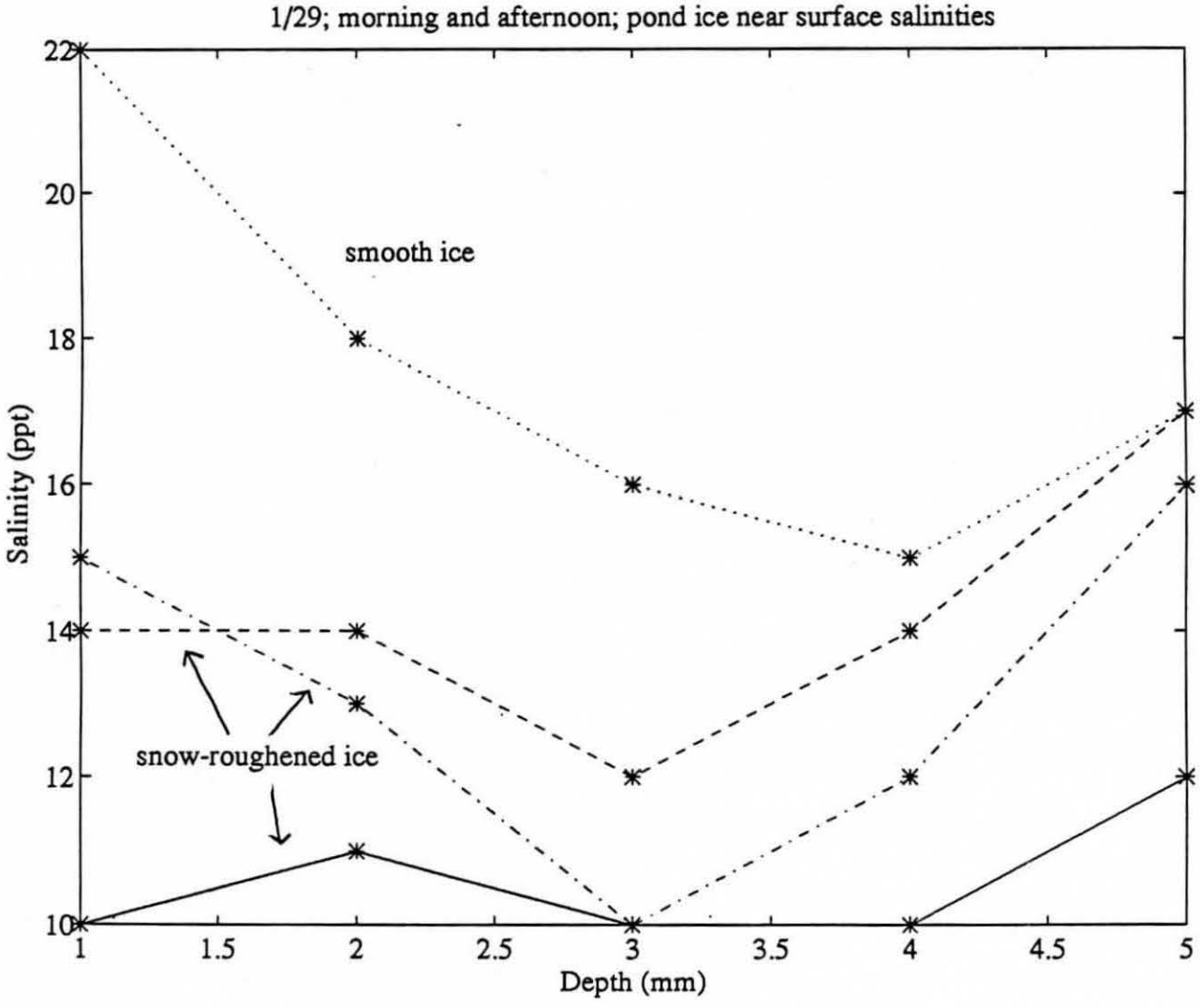
1/29; morning and afternoon; pond ice near surface salinities
Salinity (ppt)
Depth (mm)
smooth ice
snow-roughened ice
22
20
18
16
14
12
10
1
1.5
2
2.5
3
3.5
4
4.5
5

Figure 26

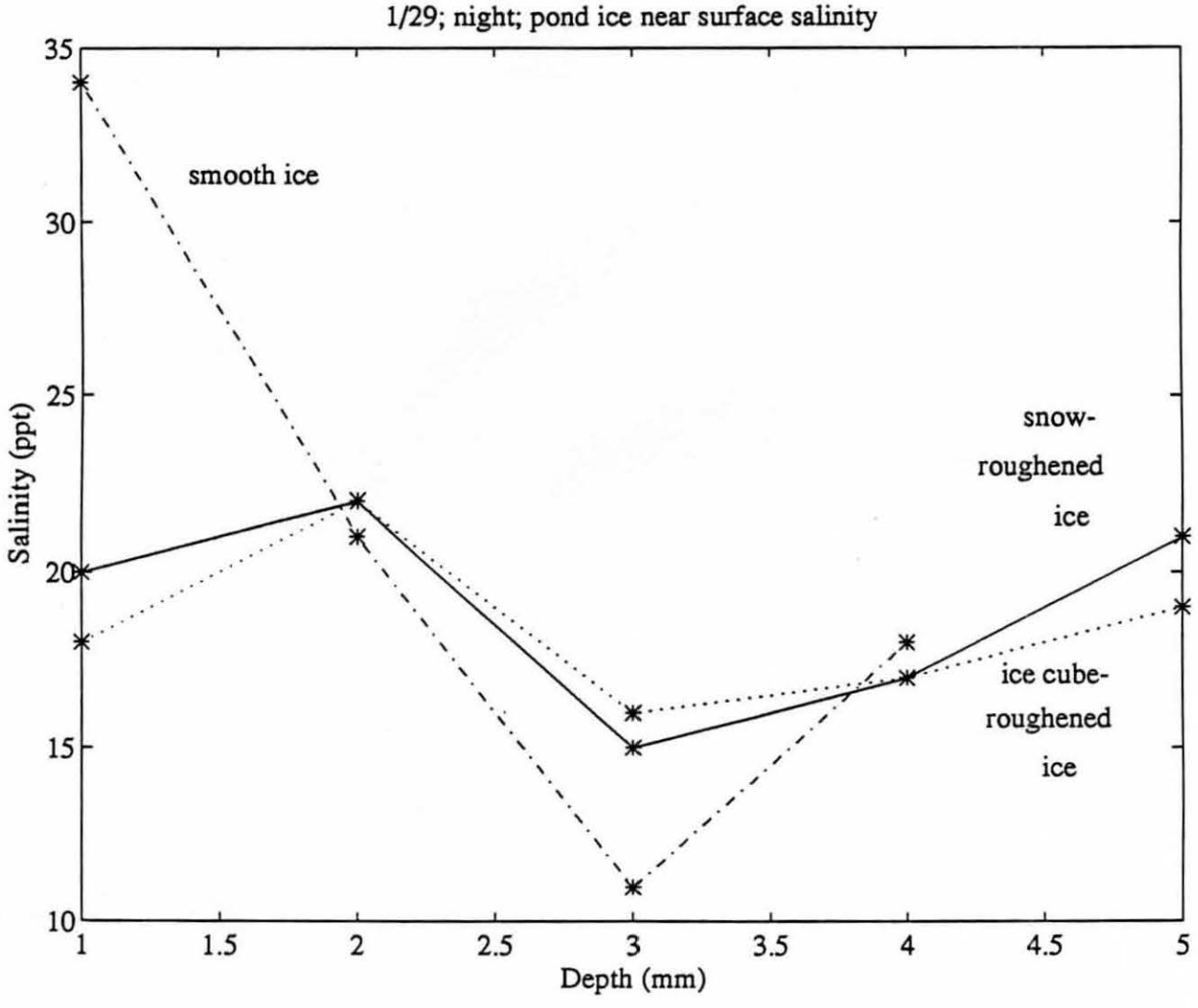
1/29; night; pond ice near surface salinity
Salinity (ppt)
Depth (mm)
smooth ice
snow-
roughened
ice
ice cube-
roughened
ice
35
30
25
20
15
10
1
1.5
2
2.5
3
3.5
4
4.5
5

Figure 27

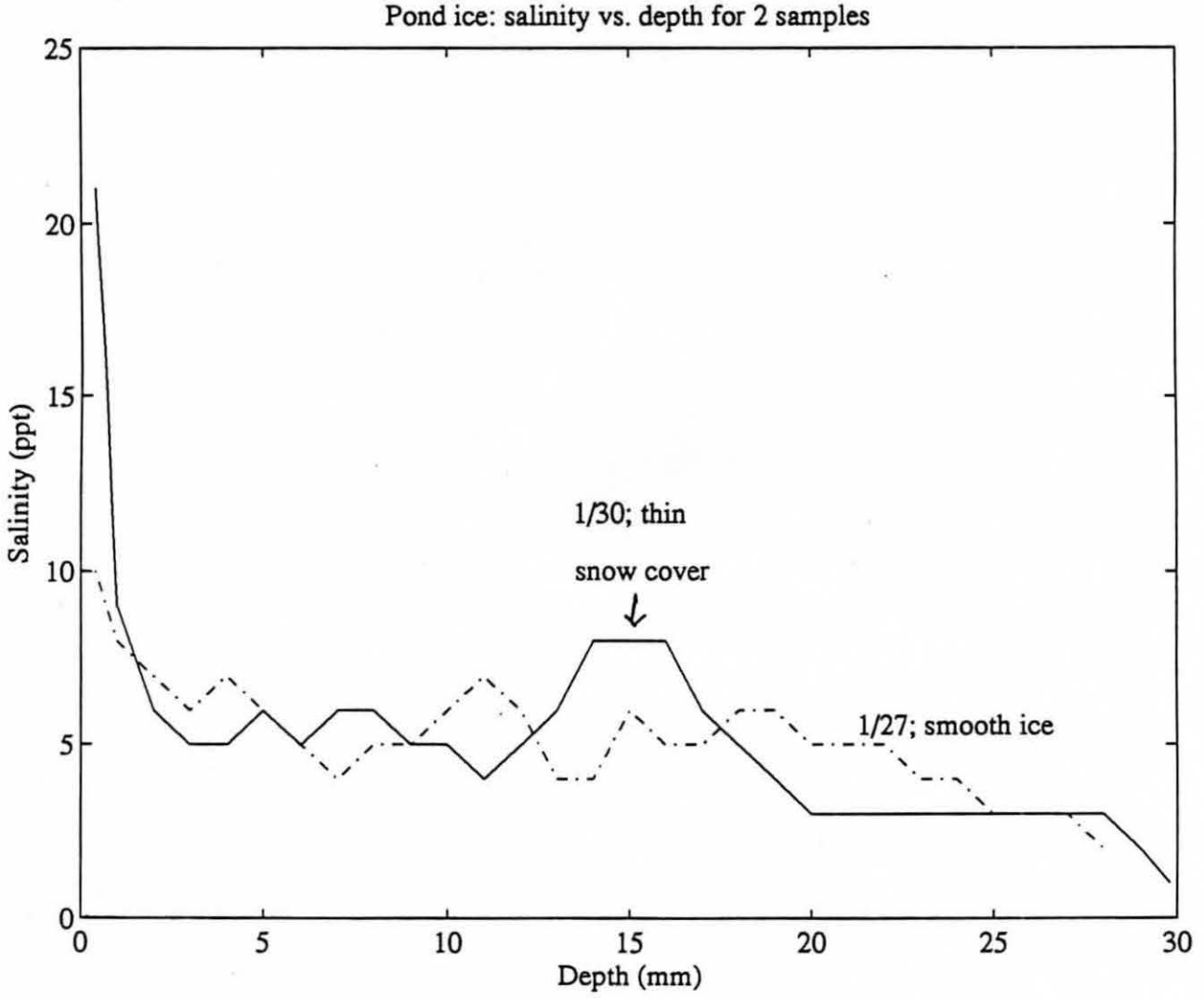
Pond ice: salinity vs. depth for 2 samples
Salinity (ppt)
Depth (mm)
1/30; thin
snow cover
1/27; smooth ice
0
5
10
15
20
25
30

Figure 28

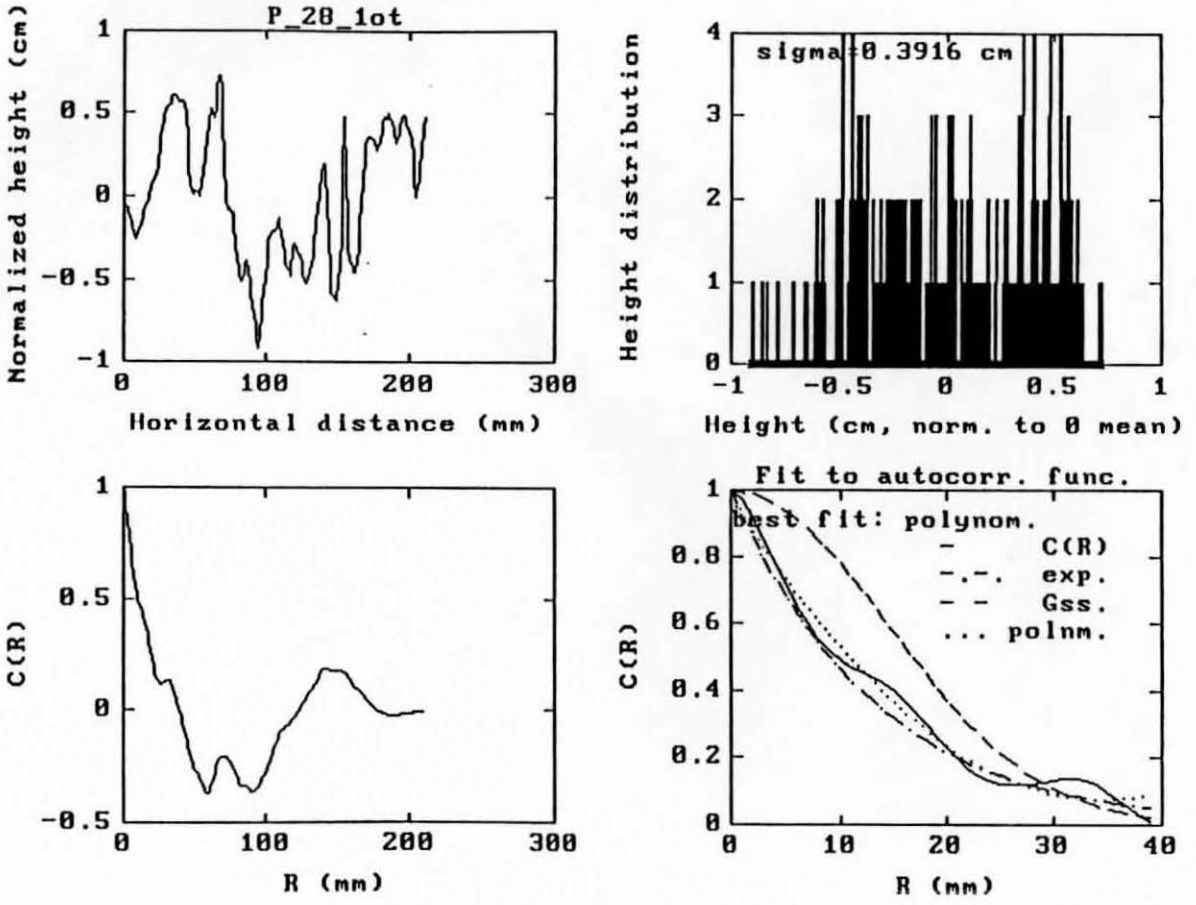

Indoor ice with ice cubes, after 2nd spraying (1/18/93)

Figure 29